Extension of Scaled Particle Theory for Rigid Disks

Martha A. Cotter and Frank H. Stillinger

Bell Telephone Laboratories, Incorporated, Murray Hill, New Jersey 07974

(Received 27 April 1972)

Geometric information about rigid disk arrangements in the plane, not previously used, is assembled and incorporated into scaled particle theory. In particular the close packed density limit for the contact correlation function $G(\lambda)$ has been obtained exactly. The revised theory provides substantially better agreement than its predecessor with molecular dynamics results for rigid disks in the fluid phase. Although high density $G(\lambda)$ curves develop nonmonotonic behavior as expected of crystalline packings, the corresponding pressure isotherms manifest no freezing transition in the present version. Suggestions for rectifying this shortcoming are included.

I. INTRODUCTION

Scaled particle theory provides a means of determining the equilibrium thermodynamic properties of a rigid particle system without first obtaining the complete pair correlation function. It was originally devised by Reiss, Frisch, and Lebowitz[1] to treat a three-dimensional fluid of rigid spheres, and has been extended to one- and two-dimensional rigid sphere fluids,[2] to mixtures of rigid spheres,[3] to isotropic fluids of hard convex particles,[4,5] and to rigid rods.[6–8] It has also been applied—in a purely formal manner—to particles with more realistic interaction potentials.[9]

A fundamental quantity in any scaled particle treatment is the reversible isothermal work W required to add a "scaled" particle with d-dimensional volume $s^d v_p$ at an arbitrary fixed point in a system of particles with volumes v_p. Closely related to W [i.e., $p_0 = \exp(-W/kT)$] is the probability p_0 that the scaled particle, added at random, will not overlap any other particle. From W or p_0 evaluated at $s=1$, an expression for any thermodynamic property as a function of density and temperature can readily be obtained. For rigid spheres or disks of diameter a, W is just the reversible work necessary to create a fixed cavity of radius λa in the system, where $\lambda = (1+s)/2$, and p_0 is just the probability of spontaneously observing such a cavity. In both cases, however, it is more convenient to formulate the theory in terms of the function $G(\lambda)$, the value of the pair correlation (radial distribution) function $g^{(2)}(r)$ upon contact between the scaled particle and a "regular" particle. By definition, $G(1) = g^{(2)}(a)$. Moreover, G is related to W or p_0 by the expressions

$$G(\lambda, \rho) = (4\pi\rho a^3 \lambda^2 kT)^{-1}[\partial W(\lambda)/\partial\lambda]$$
$$= -(4\pi\rho a^3 \lambda^2)^{-1}[\partial \ln p_0(\lambda)/\partial\lambda] \quad \text{(spheres)}[1]$$

$$\text{(1.1)}$$

and

$$G(\lambda, \rho) = (2\pi\rho a^2 \lambda kT)^{-1}[\partial W(\lambda)/\partial\lambda]$$
$$= -(2\pi\rho a^2 \lambda)^{-1}[\partial \ln p_0(\lambda)/\partial\lambda] \quad \text{(disks)},[2]$$

$$\text{(1.2)}$$

where ρ is the number density.

For both spheres and disks, the contact pair correlation function is known exactly for $\lambda \leq \frac{1}{2}$ and several exact conditions on $G(\lambda \geq \frac{1}{2}, \rho)$ have been derived.[1,2] In order to utilize this information, however, an approximate functional form for $G(\lambda)$ when $\lambda \geq \frac{1}{2}$ must be adopted. For spheres, Reiss, Frisch, and Lebowitz[1] (RFL) used

$$G(\lambda, \rho) = A(\rho) + B(\rho)/\lambda + C(\rho)/\lambda^2, \quad \text{(1.3)}$$

while Helfand, Frisch, and Lebowitz[2] (HFL) used

$$G(\lambda, \rho) = A(\rho) + B(\rho)/\lambda \quad \text{(1.4)}$$

for disks. (These forms can be shown[10] to be correct in the limit $\lambda \to \infty$.) The coefficients were then determined from the continuity properties of G at $\lambda = \frac{1}{2}$ and from the exact conditions relating $G(1)$ and $G(\infty)$. In three dimensions, this approach yields an expression for the pressure identical to that obtained from the Percus–Yevick integral equation via the Ornstein–Zernike compressibility relation.[11] In both two and three dimensions, the equation of state is in excellent agreement with numerical results[12] throughout most of the fluid range of densities. In one dimension, $G(\lambda)$ can be determined exactly[2] and leads to the known exact equation of state.

Despite these impressive results, there is clearly room for improvement in the scaled particle theories of rigid disks and spheres. First of all, in neither case is a transition to an ordered phase predicted. Rather, the RFL and HFL equations of state and contact pair correlation functions are analytic, monotonically increasing functions of ρ at all densities less than the physically unrealizable $\rho = 1/v_p$. (All four quantities are, therefore, analytic at the respective close-packed densities.) Secondly, not all the exact conditions on G which have been derived have been incorporated into the theory. For example, RFL determined but made no further use of the jump in $\partial^2 G/\partial\lambda^2$ at $\lambda = \frac{1}{2}$. More seriously, the HFL $G(\lambda)$ has, for all nonzero densities, a discontinuous slope at $\lambda = \frac{1}{2}$, whereas the exact $\partial G/\partial\lambda$ for rigid disks is known to be continuous at that point whenever $\rho < \rho_0$, the density at close packing. Finally, it is clear that additional exact conditions on $G(\lambda, \rho)$ can be derived and "put to work." These considerations,

3356

together with the substantial successes of the theory to date, suggest that further development of the scaled particle approach is a worthwhile task.

Recently, Reiss and Tully-Smith have extended scaled particle theory for rigid spheres. In the earlier[13] of two relevant papers, a new integral equation for $G(\lambda, \rho)$ was derived (through consideration of the work of cavity formation and an application of the virial theorem) and several conditions on the coefficients in an expansion of G in powers of λ^{-1} were obtained from it. Two new (approximate) equations of state were also produced, using two different functional forms for $G(\lambda \geq \frac{1}{2})$ (both of them four term power series in λ^{-1}). Later,[14] the statistical thermodynamics of curved interfaces was utilized to derive (1) an exact thermodynamic expression for $G(\lambda, \rho)$ in terms of λ, ρ, the pressure $p(\rho)$, and the quantities $\gamma_s(\lambda, \rho)$, the interfacial tension at the surface of tension outside an exclusion cavity of radius λa, and $\delta_1(\lambda, \rho)$, the distance between the surface of the cavity and the surface of tension; (2) a system of three simultaneous partial differential equations—one exact only through terms in $1/\lambda$—in the three unknowns γ_s, δ_1, and δ, where $\delta(\lambda, \rho)$ is the distance between the surface of tension and the dividing surface for which the superficial density of rigid spheres vanishes. This approach is, in a sense, complementary to that we shall employ in the present work. While Reiss and Tully-Smith were primarily concerned with large exclusion cavities, we shall concentrate on cavities of molecular dimensions, devoting particular attention to the interval $\frac{1}{2} \leq \lambda \leq 1/\sqrt{3}$. At the risk of oversimplification, it could be said that they are endeavoring to approach $\lambda = 1$ from above (they view scaled particle theory, in fact, as "an extension of macroscopic ideas into the molecular domain"), while we are attempting to reach it from below.

The remainder of this paper presents an extended scaled particle theory of rigid disks, whose primary goal is to describe that system more satisfactorily at high densities. The restriction to two dimensions greatly simplifies a number of essentially geometric arguments employed. In Sec. II, the correct limiting behavior of the contact pair correlation function at very high densities is determined. In Sec. III, a number of exact conditions are derived by expanding $G(\lambda)$ about $\lambda = \frac{1}{2}$ and—to leading order—about $\lambda = 1/\sqrt{3}$. These conditions, together with those derived previously, are then used (Sec. IV) to obtain the equation of state and expressions for $G(\lambda, \rho)$ in the intervals $\frac{1}{2} \leq \lambda < 1/\sqrt{3}$ and

$\lambda \geq 1/\sqrt{3}$. Finally, our results are presented and discussed in Sec. V, while some possible further extensions of the theory are outlined in Sec. VI.

II. THE CONTACT PAIR CORRELATION FUNCTION AT VERY HIGH DENSITY

When $\lambda < \frac{1}{2}$, the contact pair correlation function $G(\lambda, \rho)$ for rigid disks in two dimensions is given, at all densities, by[2]

$$G(\lambda, \rho) = 1/(1 - \pi\rho a^2 \lambda^2), \qquad (2.1)$$

where a is the diameter of the disks and λa is the radius of the circular region excluded to their centers by the presence of a fixed scaled particle.[15] We wish to determine how this function behaves for larger λ when the system is nearly close packed.

At the close-packed density ρ_0, the unoccupied area in the system consists solely of the three-sided "holes" in the center of triplets of disks in contact. When $\frac{1}{2} \leq \lambda \leq 1/\sqrt{3}$, the scaled particle or "λ-cule" of diameter $(2\lambda - 1)a$ will fit into such a "hole"; its center can be placed anywhere within the region labeled $\Omega_0(\lambda)$ in Fig. 1. The probability $p_0(\lambda)$ that the λ-cule can successfully be added at a randomly selected point in the system is, therefore, just the ratio of the combined area of all the regions like Ω_0 to the total area of the close-packed array. From Fig. 1, the area A_0 of Ω_0 is seen to be

$$A_0 = (\sqrt{3}a^2/4) - \tfrac{3}{2}ax - \tfrac{3}{2}\lambda^2 a^2 \phi, \qquad (2.2)$$

where

$$x = (\lambda^2 - \tfrac{1}{4})^{1/2}a \qquad (2.3)$$

and

$$\phi = \tfrac{1}{3}\pi - 2\cos^{-1}(1/2\lambda). \qquad (2.4)$$

Since, moreover,

$$a^2 \rho_0 = 2/\sqrt{3} \qquad (2.5)$$

and there are two "holes" for every disk in the system,

$$p_0(\lambda, \rho_0) = 4A_0/\sqrt{3}a^2$$

$$= 1 - 2\sqrt{3}\{(\lambda^2 - \tfrac{1}{4})^{1/2} + \lambda^2[\tfrac{1}{3}\pi - 2\cos^{-1}(1/2\lambda)]\}$$

$$(\tfrac{1}{2} \leq \lambda < 1/\sqrt{3}). \quad (2.6)$$

From (1.2), then

$$G(\lambda, \rho_0) = \frac{1 - (6/\pi)\cos^{-1}(1/2\lambda)}{1 - 2\sqrt{3}\{(\lambda^2 - \tfrac{1}{4})^{1/2} + \lambda^2[\tfrac{1}{3}\pi - 2\cos^{-1}(2\lambda)^{-1}]\}}$$

$$\tfrac{1}{2} \leq \lambda < 1/\sqrt{3}. \quad (2.7)$$

Furthermore,

$$\frac{dG(\lambda, \rho_0)}{d\lambda} = \frac{4\sqrt{3}\lambda[\tfrac{1}{3}\pi - 2\cos^{-1}(1/2\lambda)][1 - (6/\pi)\cos^{-1}(1/2\lambda)]}{(1 - 2\sqrt{3}\{(\lambda^2 - \tfrac{1}{4})^{1/2} + \lambda^2[\tfrac{1}{3}\pi - 2\cos^{-1}(1/2\lambda)]\})^2}$$

$$- \frac{3}{\pi\lambda(\lambda^2 - \tfrac{1}{4})^{1/2}(1 - 2\sqrt{3}\{(\lambda^2 - \tfrac{1}{4})^{1/2} + \lambda^2[\tfrac{1}{3}\pi - 2\cos^{-1}(1/2\lambda)]\})} \qquad \tfrac{1}{2} \leq \lambda < 1/\sqrt{3}. \quad (2.8)$$
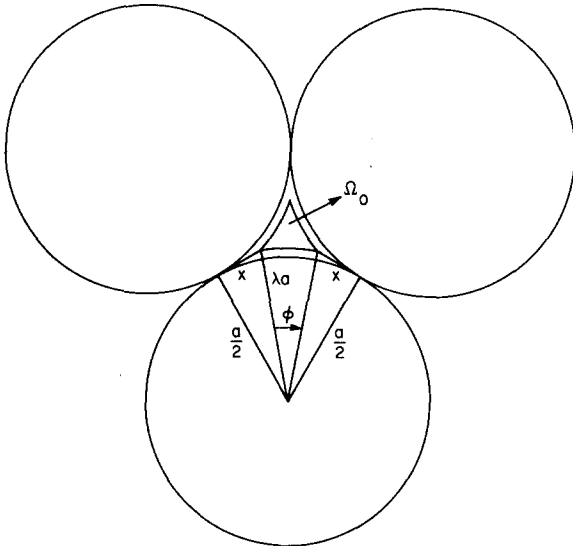
FIG. 1. A three-sided "hole" in the rigid disk close packed array. Ω_0 is the region within the "hole" available to the center of a λ-cule of diameter $(2\lambda-1)a$.

Comparing (2.7) and (2.8) with the corresponding expressions when $\lambda < \frac{1}{2}$, namely,

$$G(\lambda, \rho_0) = \frac{1}{1 - (2\pi/\sqrt{3})\lambda^2} \qquad (2.9)$$

and

$$\frac{dG(\lambda, \rho_0)}{d\lambda} = \frac{4\pi\lambda}{\sqrt{3}[1 - (2\pi/\sqrt{3})\lambda^2]^2} \qquad \lambda < \frac{1}{2}, \quad (2.10)$$

we see that $G(\lambda, \rho_0)$ is continuous at $\lambda = \frac{1}{2}$ but its slope is discontinuous and, in fact, becomes infinitely negative. $G(\lambda, \rho_0)$ clearly diverges as $\lambda \to 1/\sqrt{3}$ from below.

When $1/\sqrt{3} < \lambda < 1$, a λ-cule cannot be fitted into the perfect close packed array; but if the density is slightly less than ρ_0, there will be some vacancies present which can accommodate it. Or, alternatively, it can be forced into one of the interstices between disks, thus distorting the "crystal" structure. In Appendix A, it is argued that only monovacancies contribute to the limit function $G(\lambda, \rho_0)$ in this λ interval, since the contributions from multiple vacancies and from interstitial positions should vanish at close packing. The density ρ_{mv} of monovacancies is asymptotically given by

$$\rho_{mv}/\rho = C \exp[-C'/(\theta^{-1}-1)],^{16} \qquad (2.11)$$

where $\theta = \rho_0/\rho$ and C and C' are positive constants. Near close packing, therefore, the probability $p_0^{(mv)}(\lambda)$ that a λ-cule, "tossed" into the system at random, will be found in a monovacancy must be exceedingly small, containing, as it does, the factor ρ_{mv}/ρ. However, as λ varies within $1/\sqrt{3} < \lambda < 1$, $p_0^{(mv)}$ will undergo only modest *relative* changes, since it takes only a moderate amount of reversible work to expand a λ-cule situated within a monovacancy, where its six nearest neighbors are essentially locked into place by the remainder of

the array. In this range, then, we may set

$$p_0^{(mv)}(\lambda) = (\rho_{mv}/\rho)p_1(\lambda), \qquad (2.12)$$

and $p_1(\lambda)$ will be of order 1 near $\lambda = 1/\sqrt{3}$ and will vanish at $\lambda = 1$. (The largest λ-cule a monovacancy can contain corresponds to $\lambda = 1$.) Moreover, since $G(\lambda)$ is determined by the λ-derivative of $\ln p_0$, and only monovacancies need be considered, it is clear that $G(\lambda, \rho)$ will have a well defined limit, independent of ρ_{mv}/ρ as $\rho \to \rho_0$. At the close-packed density, $p_1(\lambda)$ is just $\rho_0 A_1(\lambda)$, where A_1 is the area of the region Ω_1 in Fig. 2; that is, $A_1(\lambda)$ is the area within a monovacancy available to the center of a λ-cule. Clearly,

$$A_1(\lambda) = (3\sqrt{3}a^2/2) - 3ax - 3\lambda^2 a^2\phi \qquad (2.13)$$

$$= (3\sqrt{3}a^2/2) - 3a^2(\lambda^2 - \tfrac{1}{4})^{1/2}$$

$$- 6\lambda^2 a^2[\tfrac{1}{3}\pi - \cos^{-1}(1/2\lambda)] \qquad 1/\sqrt{3} \leq \lambda < 1. \quad (2.14)$$

Thus,

$$G(\lambda, \rho_0)$$

$$= [-\sqrt{3}/4\pi\lambda A_1(\lambda)][dA_1(\lambda)/d\lambda] \qquad (2.15)$$

$$= \frac{2[1 - (3/\pi)\cos^{-1}(1/2\lambda)]}{3(1 - (2/\sqrt{3})\{(\lambda^2 - \tfrac{1}{4})^{1/2} + 2\lambda^2[\tfrac{1}{3}\pi - \cos^{-1}(1/2\lambda)]\})}$$

$$1/\sqrt{3} \leq \lambda < 1. \quad (2.16)$$

When $1 < \lambda < 2/\sqrt{3}$, it is necessary to find a trivacancy in order to accommodate the λ-cule. [By a trivial extension of the arguments in Appendix A, it can be seen that the contributions to $p_0(\lambda)$ and to $G(\lambda)$ from larger vacancies and from interstitial positions should be negligible for ρ slightly less than ρ_0.] $G(\lambda, \rho)$ is, therefore, determined by $\partial W^{(tv)}/\partial\lambda$, where $W^{(tv)}(\lambda, \rho)$ is the reversible isothermal work of expanding a λ-cule located within a trivancy. While the disks surrounding
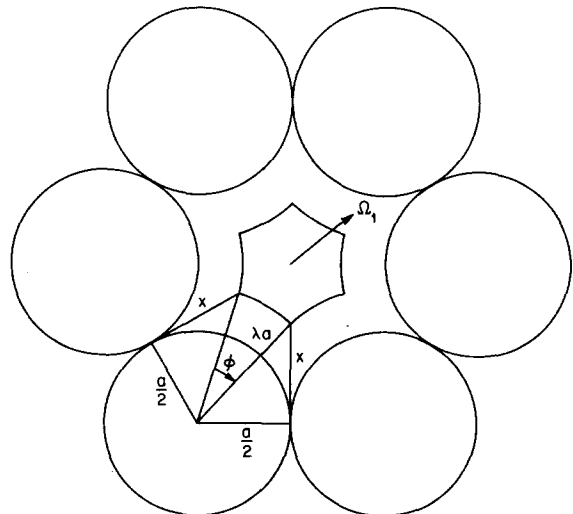

FIG. 2. A monovacancy in the highly compressed rigid disk array $(\rho \to \rho_0)$. Ω_1 is the region available to the center of a λ-cule of diameter $(2\lambda-1)a$.

a monovacancy are virtually locked into place at densities near ρ_0, the nearest neighbors of a trivancy are free to move inward, followed by motion of the second nearest neighbors, then the third nearest neighbors, etc., with the result that a λ-cule present in such a vacancy can be strongly "crowded" by its neighbors. In the limit of close packing, the number of disks in this cooperative "crowding" diverges, causing the λ-cule to experience an infinite inward mean force. (This behavior is illustrated in more detail in Appendix B.) $\partial W^{(tv)}/\partial\lambda \to \infty$, therefore, as $\rho \to \rho_0$. When $2/\sqrt{3} < \lambda < 7^{1/2}/2$, a tetravacancy must be found to accommodate the λ-cule; when $7^{1/2}/2 < \lambda < 7\sqrt{3}/9$, a 5-particle vacancy, etc. In each case, it is clear (for the reason just discussed) that $\partial W/\partial\lambda$ will diverge at close packing. Thus, the limit function $G(\lambda, \rho_0)$ does not exist for any $\lambda \geq 1$; i.e.,

$$\lim_{\rho \to \rho_0} G(\lambda, \rho) = +\infty$$

when $\lambda \geq 1$.

The three well defined branches of $G(\lambda, \rho_0)$ are shown in Fig. 3. $G(\lambda, \rho)$ for ρ somewhat less than ρ_0 should look quite similar, except that the spike near $\lambda = \frac{1}{2}$ will be rounded off and the divergences at $\lambda = 1/\sqrt{3}$ and $\lambda = 1$ replaced by maxima proportional in height to $(1/\theta - 1)^{-1}$. Beyond $\lambda = 1$, $G(\lambda)$ will be large but finite and will undoubtedly show some "structure" near $\lambda = 2/\sqrt{3}$, $\lambda = 7^{1/2}/2$, $\lambda = 7\sqrt{3}/9$, etc. The important point is that $G(\lambda)$ is strongly nonmonotonic in the ordered ("solid") phase of the rigid disk system and will almost certainly undergo a qualitative change in shape at the fluid–solid phase transition. Any truly satisfactory scaled particle theory must be able to account for this behavior.

It is far from obvious how to modify the HFL theory so that it will predict a transition to an ordered phase at high densities. However, the following points seem clear: (1) The HFL expression $G(\lambda) = A(\rho) + B(\rho)/\lambda$
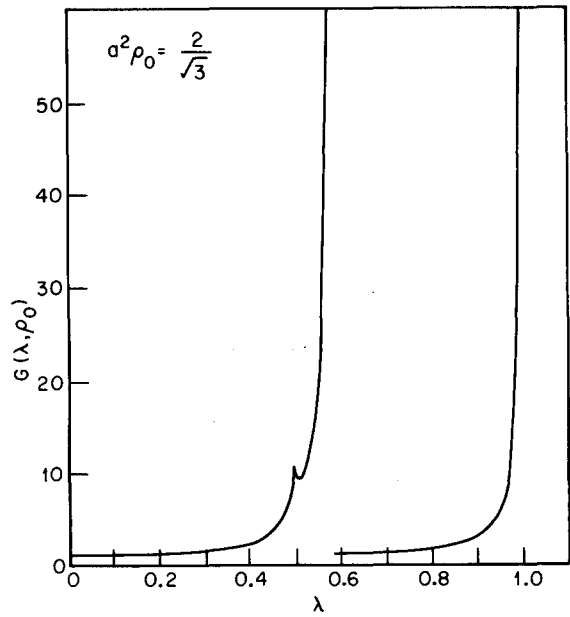

FIG. 3. The limit function $G(\lambda, \rho_0)$. For all $\lambda \geq 1$, $\lim_{\rho \to \rho_0} G(\lambda, \rho) = +\infty$.

for $\lambda > \frac{1}{2}$ is simply not flexible enough to yield the sort of nonmonotonic behavior shown in Fig. 3. (2) The use of the same approximate analytic expression for $G(\lambda)$ over the entire range of values $\lambda > \frac{1}{2}$ does not seem adequate. Ideally, one would like to use different expressions in each of the intervals $\frac{1}{2} \leq \lambda < 1/\sqrt{3}$, $1/\sqrt{3} \leq \lambda < 1$, and $\lambda \geq 1$. (3) It appears that special attention might profitably be given to the λ range near $1/\sqrt{3}$, since at that point a circular region of radius λa can first contain the centers of the triplet of disks shown in Fig. 1. Such triplets are the basic building block of the rigid disk close-packed array. With these considerations in mind, we have endeavored to produce an "improved" scaled particle theory of rigid disks.

III. EXACT CONDITIONS ON $G(\lambda, \rho)$

When $\lambda < \frac{1}{2}$, a circular region $R(\lambda)$ of radius λa can contain the center of at most one rigid disk of diameter a. The probability p_0 that such a region is empty is then just unity minus the probability that it contains one disk or

$$p_0(\lambda, \rho) = 1 - \pi\rho a^2\lambda^2 \,^{17} \qquad \lambda < \frac{1}{2}. \tag{3.1}$$

Thus,

$$G(\lambda, \rho) = -(1/2\pi\rho a^2\lambda)(\partial \ln p_0/\partial\lambda)$$

$$= (1 - \pi\rho a^2\lambda^2)^{-1} \qquad \lambda < \frac{1}{2}, \tag{3.2}$$

as noted previously. Equation (3.1) can also be obtained from the expansion

$$p_0(\lambda, \rho) = 1 + \sum_{m=1}^{\infty} \frac{(-1)^m\rho^m}{m!} \int_{[\text{region } R(\lambda) \text{ of radius } \lambda a]} \int g^{(m)}(\mathbf{r}_1, \cdots, \mathbf{r}_m) d\mathbf{r}_1 \cdots d\mathbf{r}_m \tag{3.3}$$

$$\equiv 1 + \sum_{m=1}^{\infty} (-1)^m F_m, \tag{3.4}$$

which is the two-dimensional form of the RFL Eq. (3.11).[18] When $\lambda < \frac{1}{2}$, $g^{(m)}$, the m-particle correlation function,[19]

must vanish in the circular region $R(\lambda)$ for $m \geq 2$. Therefore,

$$p_0(\lambda, \rho) = 1 - F_1 = 1 - \rho \int_{R(\lambda)} g^{(1)}(\mathbf{r}_1) d\mathbf{r}_1$$

$$= 1 - \pi \rho a^2 \lambda^2 \qquad \lambda < \tfrac{1}{2}. \tag{3.5}$$

Furthermore, for $\tfrac{1}{2} \leq \lambda < 1/\sqrt{3}$, $R(\lambda)$ can contain the center of at most two rigid disks; hence $F_m = 0$ for $m \geq 3$ and

$$p_0(\lambda, \rho) = 1 - F_1 + F_2$$

$$= 1 - \pi \rho a^2 \lambda^2 + \tfrac{1}{2} \rho^2 \int_{R(\lambda)} d\mathbf{r}_1 \int_{R(\lambda)} d\mathbf{r}_2 g^{(2)}(\mathbf{r}_1, \mathbf{r}_2, \rho) \qquad \tfrac{1}{2} \leq \lambda < 1/\sqrt{3}. \tag{3.6}$$

As it stands, (3.6) clearly has no computational utility. It can be used, however, to obtain expansions of p_0 and G about $\lambda = \tfrac{1}{2}$.

The integral F_2 may be rewritten as[20]

$$F_2 = \tfrac{1}{2} \rho^2 2\pi \int_{(1-\lambda)a}^{\lambda a} r_1 dr_1 \int_a^{(r_1+\lambda a)} 2\theta_m(r_1, r_2, \lambda) g^{(2)}(r_{12}, \rho) r_{12} dr_{12}, \tag{3.7}$$

where the meaning of the various coordinates can be seen from Fig. 4. $[(1-\lambda)a$ is the minimum value r_1 can attain if disk 2 is to remain within the circular region.$]$ Clearly, θ_m, the maximum allowable value of θ for a given λ, r_1, and r_{12}, is given by

$$\cos\theta_m = (r_1^2 + r_{12}^2 - \lambda^2 a^2)/2r_1 r_{12} \tag{3.8}$$

$$= (s_1^2 + s_{12}^2 - \lambda^2)/2s_1 s_{12}, \tag{3.9}$$

where

$$s_1 = r_1/a,$$

$$s_{12} = r_{12}/a. \tag{3.10}$$

Therefore,

$$F_2 = 2\pi(\rho a^2)^2 \int_{(1-\lambda)}^{\lambda} s_1 ds_1 \int_1^{(s_1+\lambda)} s_{12} \cos^{-1}\left(\frac{s_1^2 + s_{12}^2 - \lambda^2}{2s_1 s_{12}}\right) g^{(2)}(as_{12}, \rho) ds_{12}. \tag{3.11}$$

When λ is only slightly greater than $\tfrac{1}{2}$, s_{12} is confined to a narrow range of values ≥ 1. Thus we can write

$$F_2 = 2\pi(\rho a^2)^2 \int_{(1-\lambda)}^{\lambda} s_1 ds_1 \int_1^{(s_1+\lambda)} s_{12} \cos^{-1}\left(\frac{s_1^2 + s_{12}^2 - \lambda^2}{2s_1 s_{12}}\right) \left\{ G(1, \rho) + \left[\frac{\partial g^{(2)}(as_{12}, \rho)}{\partial s_{12}}\right]_{s_{12}=1} (s_{12} - 1) \right.$$
$$\left. + \frac{1}{2}\left[\frac{\partial^2 g^{(2)}(as_{12}, \rho)}{\partial s_{12}^2}\right]_{s_{12}=1} (s_{12} - 1)^2 + \cdots \right\} ds_{12} \tag{3.12}$$

$$= 2\pi(\rho a^2)^2 \int_{(1-\lambda)}^{\lambda} s_1 ds_1 \int_0^{(s_1+\lambda-1)} (s_1 + \lambda - t) \cos^{-1}\left[\frac{s_1^2 - \lambda^2 + (s_1+\lambda-t)^2}{2s_1(s_1+\lambda-t)}\right] \left\{ G(1, \rho) + \left(\frac{\partial g^{(2)}}{\partial s_{12}}\right)_{s_{12}=1} (s_1 + \lambda - 1 - t) \right.$$
$$\left. + \frac{1}{2}\left(\frac{\partial^2 g^{(2)}}{\partial s_{12}^2}\right)_{s_{12}=1} (s_1 + \lambda - 1 - t)^2 + \cdots \right\} dt, \tag{3.13}$$

if we introduce the small quantity

$$t = s_1 + \lambda - s_{12}. \tag{3.14}$$

Expanding the argument of the inverse cosine in powers of t and utilizing the series

$$\cos^{-1}(1 - \tfrac{1}{2}x^2) = x + (x^3/24) + (3x^5/640) + \cdots, \tag{3.15}$$

it can be shown that

$$\cos^{-1}\left[\frac{s_1^2 - \lambda^2 + (s_1+\lambda-t)^2}{2s_1(s_1+\lambda-t)}\right] = \left[\frac{2\lambda t}{s_1(s_1+\lambda)}\right]^{1/2}\left\{ 1 + \left[\frac{1}{12} + \frac{s_1(\lambda-s_1)}{4\lambda^2}\right]\frac{\lambda t}{s_1(s_1+\lambda)} \right.$$
$$\left. + \left[\frac{3}{160} + \frac{s_1(\lambda-s_1)}{16\lambda^2} + \frac{s_1^2(\lambda-s_1)}{4\lambda^3} - \frac{s_1^2(\lambda-s_1)^2}{32\lambda^4}\right]\frac{\lambda^2 t^2}{s_1^2(s_1+\lambda)^2} + O(t^3) \right\} \tag{3.16}$$

$$\equiv (2t)^{1/2}[A_0(s_1, \lambda) + A_1(s_1, \lambda)t + A_2(s_1, \lambda)t^2 + O(t^3)]. \tag{3.17}$$

Then, (3.17) can be substituted into (3.13) and the integration over t performed to give—after considerable

rearrangement—

$$F_2 = 4\sqrt{2}\pi(\rho a^2)^2 \int_{(1-\lambda)}^{\lambda} s_1\{\tfrac{1}{3}(s_1+\lambda)A_0(s_1,\lambda)G(1,\rho)(s_1+\lambda-1)^{3/2}$$

$$+\tfrac{1}{5}\{[(s_1+\lambda)A_1(s_1,\lambda)-A_0(s_1,\lambda)]G(1,\rho)+\tfrac{2}{3}(s_1+\lambda)A_0(s_1,\lambda)(\partial g^{(2)}/\partial s_{12})_{s_{12}=1}\}(s_1+\lambda-1)^{5/2}$$

$$+\tfrac{1}{7}\{[(s_1+\lambda)A_2(s_1,\lambda)-A_1(s_1,\lambda)]G(1,\rho)+\tfrac{2}{5}[(s_1+\lambda)A_1(s_1,\lambda)-A_0(s_1,\lambda)](\partial g^{(2)}/\partial s_{12})_{s_{12}=1}$$

$$+(4/15)(s_1+\lambda)A_0(s_1,\lambda)(\partial^2 g^{(2)}/\partial s_{12}^2)_{s_{12}=1}\}(s_1+\lambda-1)^{7/2}+O[(s_1+\lambda-1)^{9/2}]\}ds_1. \quad (3.18)$$

At this point, it is convenient to change the variable of integration from s_1 to ζ, where

$$\zeta = s_1+\lambda-1. \quad (3.19)$$

Then, we can expand s_1, A_0, A_1, and A_2 in powers of ζ, insert the expansions in the integrand of (3.18), integrate from $\zeta=0$ to $\zeta=2\lambda-1$, and collect like powers of $(\lambda-\tfrac{1}{2})$ to obtain

$$F_2 = \frac{32\sqrt{2}\pi(\rho a^2)^2\lambda^{1/2}}{15}\left\{G(1,\rho)(\lambda-\tfrac{1}{2})^{5/2}+\frac{2}{7}\left[(1+\tfrac{1}{2}\lambda)G(1,\rho)+2a\left(\frac{\partial g^{(2)}}{\partial r_{12}}\right)_{r_{12}=a}\right](\lambda-\tfrac{1}{2})^{7/2}\right.$$

$$\left.+\frac{2}{21}\left[\frac{[1+\tfrac{4}{3}\lambda-(11/3)\lambda^2+\tfrac{3}{4}\lambda^3]G(1,\rho)}{\lambda}+4(1+\tfrac{1}{6}\lambda)a\left(\frac{\partial g^{(2)}}{\partial r_{12}}\right)_{r_{12}=a}+\frac{8}{3}a^2\left(\frac{\partial^2 g^{(2)}}{\partial r_{12}^2}\right)_{r_{12}=a}\right](\lambda-\tfrac{1}{2})^{9/2}+O[(\lambda-\tfrac{1}{2})^{11/2}]\right\}. \quad (3.20)$$

Finally, expanding the various functions of λ in (3.20) in powers of $(\lambda-\tfrac{1}{2})$ and rearranging yields the desired expression for F_2:

$$F_2 = \frac{32\pi(\rho a^2)^2}{15}\left\{G(1,\rho)(\lambda-\tfrac{1}{2})^{5/2}+\frac{4}{7}\left[a\left(\frac{\partial g^{(2)}}{\partial r_{12}}\right)_{r_{12}=a}+\frac{19}{8}G(1,\rho)\right](\lambda-\tfrac{1}{2})^{7/2}\right.$$

$$\left.+\frac{16}{63}\left[a^2\left(\frac{\partial^2 g^{(2)}}{\partial r_{12}^2}\right)_{r_{12}=a}+\frac{31}{8}a\left(\frac{\partial g^{(2)}}{\partial r_{12}}\right)_{r_{12}=a}+\frac{81}{128}G(1,\rho)\right](\lambda-\tfrac{1}{2})^{9/2}+\cdots\right\}. \quad (3.21)$$

Furthermore, $G(\lambda,\rho)$ can now be determined through terms proportional to $(\lambda-\tfrac{1}{2})^{7/2}$, since

$$G(\lambda,\rho) = -(2\pi\rho a^2\lambda)^{-1}\frac{\partial \ln p_0}{\partial \lambda} = \frac{1-(1/2\pi\rho a^2\lambda)(\partial F_2/\partial \lambda)}{1-\pi\rho a^2\lambda^2+F_2(\lambda,\rho)} \quad (3.22)$$

$$= \frac{[1-(1/2\pi\rho a^2\lambda)(\partial F_2/\partial \lambda)][1-F_2/(1-\pi\rho a^2\lambda^2)+\cdots]}{(1-\pi\rho a^2\lambda^2)}. \quad (3.23)$$

Substituting $\partial F_2/\partial \lambda$ [from (3.21)], together with expansions of λ^{-1} and $(1-\pi\rho a^2\lambda^2)^{-1}$ in powers of $(\lambda-\tfrac{1}{2})$, into (3.23) leads—after much tedious algebra—to

$$G(\lambda,\rho) = (1-\pi a^2\lambda^2\rho)^{-1}-\frac{16a^2\rho}{3(1-\tfrac{1}{4}\pi a^2\rho)}\left\{G(1,\rho)(\lambda-\tfrac{1}{2})^{3/2}+\left[\tfrac{4}{5}a\left(\frac{\partial g^{(2)}}{\partial r_{12}}\right)_{r_{12}=a}-\frac{[1-(57/4)\pi a^2\rho]G(1,\rho)}{10(1-\tfrac{1}{4}\pi a^2\rho)}\right](\lambda-\tfrac{1}{2})^{5/2}\right.$$

$$+\left[\frac{16}{35}a^2\left(\frac{\partial^2 g^{(2)}}{\partial r_{12}^2}\right)_{r_{12}=a}+\frac{6}{35}\frac{[1+(23/4)\pi a^2\rho]}{(1-\tfrac{1}{4}\pi a^2\rho)}\left(\frac{\partial g^{(2)}}{\partial r_{12}}\right)_{r_{12}=a}\right.$$

$$\left.\left.+\frac{137}{280}\frac{[1+(671/274)\pi a^2\rho+(6585/2192)\pi^2 a^4\rho^2]G(1,\rho)}{(1-\tfrac{1}{4}\pi a^2\rho)^2}\right](\lambda-\tfrac{1}{2})^{7/2}+\cdots\right\}. \quad (3.24)$$

We shall make extensive use of this relation in Sec. IV. From (3.24) it is clear that both $G(\lambda)$ and $\partial G/\partial \lambda$ are continuous at $\lambda=\tfrac{1}{2}$, (when $\rho<\rho_0$) but that $\partial^2 G/\partial \lambda^2$ is discontinuous and, in fact, diverges as $(\lambda-\tfrac{1}{2})^{-1/2}$. In Appendix C, moreover, $F_3(\lambda,\rho)$ is expanded to leading order in powers of $(\lambda-1/\sqrt{3})$ and it is shown that G and its first three derivatives with respect to λ are continuous at $\lambda=1/\sqrt{3}$ ($\rho<\rho_0$) while $\partial^4 G/\partial \lambda^4$ is discontinuous there. All this provides information concerning the

behavior of the exact $G(\lambda,\rho)$.[21] In addition, it has recently been shown[10] that G for large λ can be expanded in nonnegative integral powers of λ^{-1}, and that the coefficient of λ^{-2} in this series is identically zero. Finally, two more exact conditions on the contact correlation function are known[1,2]: the so-called integral and infinity conditions. Brief derivations of both of them are given below.

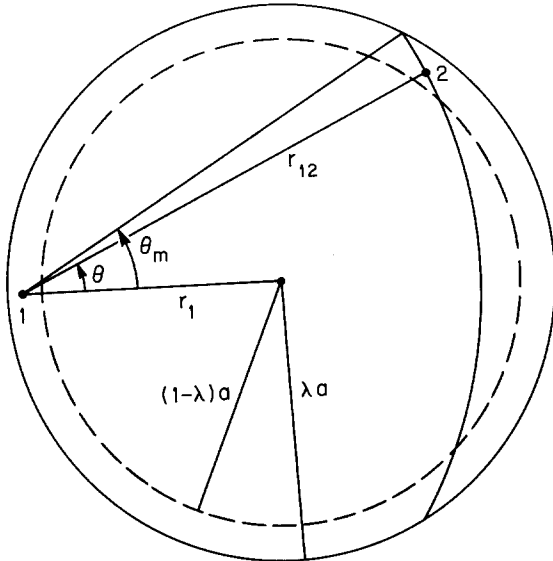From the definition of the reversible work $W(\lambda,\rho)$,

FIG. 4. A circular region of radius λa. Points 1 and 2 represent the centers of rigid disks 1 and 2, respectively, both of diameter a.

it is clear that $W(1, \rho)$ is the change in Helmholtz free energy—at constant T and V—upon placing an additional disk of diameter a in the system at some fixed point. The chemical potential μ in the rigid disk assembly is, therefore, just $W(1, \rho)$ plus a free energy of mixing term, or

$$\mu/kT = \ln(\rho\Lambda^2) + [W(1, \rho)/kT], \qquad (3.25)$$

where Λ^2 is the reciprocal of the (particle) translational momentum partition function. From (1.2), however, it can be seen that

$$\frac{W(1, \rho)}{kT} = 2\pi\rho a^2 \int_0^1 \lambda G(\lambda, \rho) \, d\lambda; \qquad (3.26)$$

hence,

$$\frac{\mu}{kT} = \ln(\rho\Lambda^2) + 2\pi\rho a^2 \int_0^1 \lambda G(\lambda, \rho) \, d\lambda. \qquad (3.27)$$

Substituting (3.27) into the thermodynamic relation

$$p = \int_0^\rho \rho' \left(\frac{\partial\mu}{\partial\rho'}\right)_T d\rho' \qquad (3.28)$$

and integrating by parts yields

$$\frac{p}{kT} = \rho + \rho^2 a^2 \int_0^1 2\pi\lambda G(\lambda, \rho) \, d\lambda$$

$$- a^2 \int_0^\rho \rho' d\rho' \int_0^1 2\pi\lambda G(\lambda, \rho') \, d\lambda. \qquad (3.29)$$

Finally, equating the right-hand side of (3.29) with the right-hand side of the well-known expression for the equation of state of rigid disks; namely,

$$p/kT = \rho + \tfrac{1}{2}\pi\rho^2 a^2 g^{(2)}(a, \rho)$$

$$\equiv \rho + \tfrac{1}{2}\pi\rho^2 a^2 G(1, \rho), \qquad (3.30)$$

we obtain the integral condition

$$\tfrac{1}{2}\rho^2 G(1, \rho) = 2\rho^2 \int_0^1 \lambda G(\lambda, \rho) \, d\lambda$$

$$- 2 \int_0^\rho \rho' d\rho' \int_0^1 \lambda G(\lambda, \rho') \, d\lambda. \qquad (3.31)$$

For very large λ, $W(\lambda, \rho)$ is the work of creating a macroscopic cavity in the system, and $\rho G(\lambda, \rho)$ is the average density of disks (of diameter a) in contact with the outer surface of such a cavity. In the limit $\lambda \to \infty$, this surface becomes a hard flat wall with which the disks impulsively collide. Since the stress normal to the wall is purely kinetic, we can write

$$p/kT = \rho G(\infty, \rho), \qquad (3.32)$$

where p is the hydrostatic pressure. Equation (3.32), together with Eq. (3.30), yields the infinity condition

$$G(\infty, \rho) = 1 + \tfrac{1}{2}\pi\rho a^2 G(1, \rho). \qquad (3.33)$$

IV. EXPRESSIONS FOR $G(\lambda, \rho)$ AND THE EQUATION OF STATE

In this section, our task is to utilize the exact conditions presented in Sec. III in order to obtain (approximate) expressions for $G(\lambda, \rho)$ in the various λ intervals with $\lambda \geq \tfrac{1}{2}$. As was noted previously, one would like—given Fig. 3—to use a different functional form for G in each of the intervals $\tfrac{1}{2} \leq \lambda < 1/\sqrt{3}$, $1/\sqrt{3} \leq \lambda < 1$, and $\lambda \geq 1$. Toward that end, the small interval $\tfrac{1}{2} \leq \lambda < 1/\sqrt{3}$ can probably be spanned satisfactorily by the first few terms in (3.24); moreover, it is likely that a Laurent series in nonpositive powers of λ can safely be used for $\lambda \geq 1$, since such a series is asymptotically correct for large λ[10] and is not—as was demonstrated by HFL—a bad approximation even for $\tfrac{1}{2} \leq \lambda < 1$. The middle interval $1/\sqrt{3} \leq \lambda < 1$, however, causes certain problems. First of all, although $G(\lambda)$ can be expanded about $\lambda = 1/\sqrt{3}$ (see Appendix C) it seems unlikely that the resulting series can adequately span the entire interval without retaining more terms than there are exact conditions to determine the coefficients. Furthermore, an expansion about $\lambda = 1/\sqrt{3}$ may well be a really good approximation only in the range $1/\sqrt{3} \leq \lambda < 1/\sqrt{2}$, since at $\lambda = 1/\sqrt{2}$ four disks of diameter a (in a square configuration) can just fit into a region $R(\lambda)$ of radius λa and some derivative $\partial^m G/\partial\lambda^m$ $(m \geq 5)$ will, therefore, be discontinuous.[22] Similarly some higher λ derivative of G will be discontinuous at $\lambda = [2/(5-5^{1/2})]^{1/2}$, the point at which $R(\lambda)$ can just contain 5 disks of diameter a in a pentagonal configuration.[23] To avoid these difficulties, we have undertaken the somewhat less ambitious program of dividing the interval $\lambda \geq \tfrac{1}{2}$ into only two subintervals: $\tfrac{1}{2} \leq \lambda < 1/\sqrt{3}$ and $\lambda \geq 1/\sqrt{3}$. The resulting $G(\lambda \geq 1/\sqrt{3})$ will probably not have the correct slope and curvature near $\lambda = 1$ at very high densities. In order to obtain a satisfactory equation of state, however, it is sufficient, in principle, to know $G(\lambda, \rho)$ very

accurately in the range $\frac{1}{2} \leq \lambda < 1/\sqrt{3}$, since the coefficient of $(\lambda - \frac{1}{2})^{3/2}$ in (3.24) is a linear function of $G(1, \rho)$. [Recall Eq. (3.30).]

The expression for G we shall use in the interval $\frac{1}{2} \leq \lambda < 1/\sqrt{3}$ is

$$G(\lambda, y) = (1 - \tfrac{1}{4}y)^{-1} + [y/(1 - \tfrac{1}{4}y)^2](\lambda - \tfrac{1}{2})$$
$$- C_1(y)(\lambda - \tfrac{1}{2})^{3/2} + [y(1 + \tfrac{3}{4}y)/(1 - \tfrac{1}{4}y)^3](\lambda - \tfrac{1}{2})^2$$
$$- C_2(y)(\lambda - \tfrac{1}{2})^{5/2} + [2y^2(1 + \tfrac{1}{4}y)/(1 - \tfrac{1}{4}y)^4](\lambda - \tfrac{1}{2})^3$$
$$- C_3(y)(\lambda - \tfrac{1}{2})^{7/2} \qquad \tfrac{1}{2} \leq \lambda < \sqrt{3}^{-1}, \quad (4.1)$$

where

$$y = \pi a^2 \rho \qquad (4.2)$$

and $(-C_1)$, $(-C_2)$, and $(-C_3)$ are the coefficients of $(\lambda - \frac{1}{2})^{3/2}$, $(\lambda - \frac{1}{2})^{5/2}$, and $(\lambda - \frac{1}{2})^{7/2}$, respectively, in (3.24).[24] Clearly, (4.1) was obtained from (3.24) by expanding $(1 - \pi a^2 \lambda^2 \rho)$ in powers of $(\lambda - \frac{1}{2})$ and truncating the series after the term in $(\lambda - \frac{1}{2})^3$. Failure to perform this expansion would lead to an equation of state with an unwanted divergence at $y = 3$.

Section II provides us with seven exact conditions on G and there are three coefficients to be determined in (4.1). Therefore, we could use for $G(\lambda \geq 1/\sqrt{3})$ the first four terms of the aforementioned Laurent series

$$G(\lambda, y) = A_0(y) + [A_1(y)/\lambda]$$
$$+ [A_3(y)/\lambda^3] + [A_4(y)/\lambda^4] + \cdots. \quad (4.3)$$

(A_2 must be identically zero.[10]) Instead, however, we shall adopt the somewhat more general expression

$$G(\lambda, y) = A(y) + [B(y)/\lambda] + [D(y)/(\lambda - \lambda_3)^3]$$
$$+ [E(y)/(\lambda - \lambda_4)^4] \qquad \lambda \geq 1/\sqrt{3}, \quad (4.4)$$

where λ_3 and λ_4 are constants. [We shall construct the function $G(\lambda, y)$ for a number of different pairs (λ_3, λ_4).] There are two principle reasons for this choice: (1) To obtain a really good approximation to the exact $G(\lambda)$, four terms in (4.3) are probably insufficient for λ of order unity; with the proper λ_3 and λ_4 we can compensate to some extent for the omission of higher order terms. (2) It is hoped that for certain values of λ_3 and/or λ_4 reasonably close to $1/\sqrt{3}$, a rapid variation in the high density $G(\lambda)$ will occur as $\lambda \to 1/\sqrt{3}$ from above—in agreement with the behavior shown in Fig. 3. In the end, of course, the introduction of λ_3 and λ_4 must be justified by the results to which it leads. Finally, let us note that the coefficient $A(y)$ gives, in fact, the equation of state since, from (3.3) and (4.4),

$$p/\rho kT = G(\infty) = A. \qquad (4.5)$$

Equating $G(\lambda = 1/\sqrt{3})$, $(\partial G/\partial \lambda)_{\lambda = 1/\sqrt{3}}$, $(\partial^2 G/\partial \lambda^2)_{\lambda = 1/\sqrt{3}}$, and $(\partial^3 G/\partial \lambda^3)_{\lambda = 1/\sqrt{3}}$ from (4.1) with the corresponding expressions obtained from (4.4), yields the following relations:

$$A + \sqrt{3}B + \frac{D}{(1/\sqrt{3} - \lambda_3)^3} + \frac{E}{(1/\sqrt{3} - \lambda_4)^4} = (1 - \tfrac{1}{4}y)^{-1} + \frac{n^2 y}{(1 - \tfrac{1}{4}y)^2} + \frac{n^4 y(1 + \tfrac{3}{4}y)}{(1 - \tfrac{1}{4}y)^3} + \frac{2n^6 y^2(1 + \tfrac{1}{4}y)}{(1 - \tfrac{1}{4}y)^4} - n^3 C_1 - n^5 C_2 - n^7 C_3,$$
$$(4.6)$$

$$3B + \frac{3D}{(1/\sqrt{3} - \lambda_3)^4} + \frac{4E}{(1/\sqrt{3} - \lambda_4)^5} = \frac{-y}{(1 - \tfrac{1}{4}y)^2} - \frac{2n^2 y(1 + \tfrac{3}{4}y)}{(1 - \tfrac{1}{4}y)^3} - \frac{6n^4 y^2(1 + \tfrac{1}{4}y)}{(1 - \tfrac{1}{4}y)^4} + \tfrac{3}{2}nC_1 + \tfrac{5}{2}n^3 C_2 + \tfrac{7}{2}n^5 C_3, \quad (4.7)$$

$$6\sqrt{3}B + \frac{12D}{(1/\sqrt{3} - \lambda_3)^5} + \frac{20E}{(1/\sqrt{3} - \lambda_4)^6} = \frac{2y(1 + \tfrac{3}{4}y)}{(1 - \tfrac{1}{4}y)^3} + \frac{12n^2 y^2(1 + \tfrac{1}{4}y)}{(1 - \tfrac{1}{4}y)^4} - \frac{3}{4}\frac{C_1}{n} - \tfrac{15}{4}nC_2 - \tfrac{35}{4}n^3 C_3, \quad (4.8)$$

$$54B + \frac{60D}{(1/\sqrt{3} - \lambda_3)^6} + \frac{120E}{(1/\sqrt{3} - \lambda_4)^7} = \frac{-12y^2(1 + \tfrac{1}{4}y)}{(1 - \tfrac{1}{4}y)^4} - \frac{3}{8}\frac{C_1}{n^3} + \frac{15}{8}\frac{C_2}{n} + \tfrac{105}{8}nC_3, \quad (4.9)$$

where

$$n = (1/\sqrt{3} - \tfrac{1}{2})^{1/2}.$$

Furthermore, in terms of the coefficients A, B, D, E, C_1, C_2, C_3, and the variable y, the infinity condition, the definition of C_1 as a function of $G(1)$, and the integral condition become, respectively,

$$A = 1 + (3\pi/32)(1 - \tfrac{1}{4}y)C_1, \qquad (4.10)$$

$$A + B + \frac{D}{(1 - \lambda_3)^3} + \frac{E}{(1 - \lambda_4)^4} = \frac{3\pi(1 - \tfrac{1}{4}y)C_1}{16y}, \qquad (4.11)$$

$$y(A - 1) = 2y^2 \left[\int_0^{1/2} \frac{\lambda d\lambda}{(1 - y\lambda^2)} + \int_{1/2}^{1/\sqrt{3}} \lambda G(\tfrac{1}{2} \leq \lambda < 1/\sqrt{3}) d\lambda + \int_{1/\sqrt{3}}^{1} \lambda G(\lambda \geq 1/\sqrt{3}) d\lambda \right]$$
$$- 2 \int_0^y y' dy' \left[\int_0^{1/2} \frac{\lambda d\lambda}{(1 - y'\lambda^2)} + \int_{1/2}^{1/\sqrt{3}} \lambda G(\tfrac{1}{2} \leq \lambda < 1/\sqrt{3}, y') d\lambda + \int_{1/\sqrt{3}}^{1} \lambda G(\lambda \geq 1/\sqrt{3}, y') d\lambda \right] \quad (4.12)$$

$$= -4\ln(1-\tfrac{1}{4}y) - y + 2y^2 \left\{ [24(1-\tfrac{1}{4}y)]^{-1} + \frac{n^4(1+\tfrac{4}{5}n^2)y}{4(1-\tfrac{1}{4}y)^2} + \frac{n^6(1+\tfrac{3}{2}n^2)(1+\tfrac{3}{4}y)y}{6(1-\tfrac{1}{4}y)^3} + \frac{n^8(1+\tfrac{8}{5}n^2)y^2(1+\tfrac{1}{4}y)}{4(1-\tfrac{1}{4}y)^4} \right.$$

$$-\tfrac{1}{5}n^5(1+\tfrac{10}{7}n^2)C_1 - \tfrac{1}{7}n^7(1+\tfrac{14}{9}n^2)C_2 - \tfrac{1}{9}n^9(1+\tfrac{18}{11}n^2)C_3 + \tfrac{1}{3}A + (1-1/\sqrt3)B + \left[\frac{(2/\sqrt3)-\lambda_3}{(1/\sqrt3-\lambda_3)^2} - \frac{(2-\lambda_3)}{(1-\lambda_3)^2} \right]\tfrac{1}{2}D$$

$$+ \left[\frac{\sqrt3-\lambda_4}{(1/\sqrt3-\lambda_4)^3} - \frac{(3-\lambda_4)}{(1-\lambda_4)^3} \right]\tfrac{1}{6}E \right\} - 2\int_0^y y' \left\{ [24(1-\tfrac{1}{4}y')]^{-1} + \frac{n^4(1+\tfrac{4}{5}n^2)y'}{4(1-\tfrac{1}{4}y')^2} + \frac{n^6(1+\tfrac{3}{2}n^2)y'(1+\tfrac{3}{4}y')}{6(1-\tfrac{1}{4}y')^3} \right.$$

$$+ \frac{n^8(1+\tfrac{8}{5}n^2)y'^2(1+\tfrac{1}{4}y')}{4(1-\tfrac{1}{4}y')^4} - \tfrac{1}{5}n^5(1+\tfrac{10}{7}n^2)C_1 - \tfrac{1}{7}n^7(1+\tfrac{14}{9}n^2)C_2 - \tfrac{1}{9}n^9(1+\tfrac{18}{11}n^2)C_3 + \tfrac{1}{3}A + (1-1/\sqrt3)B$$

$$\left. + \left[\frac{(2/\sqrt3)-\lambda_3}{(1/\sqrt3-\lambda_3)^2} - \frac{(2-\lambda_3)}{(1-\lambda_3)^2} \right]\tfrac{1}{2}D + \left[\frac{\sqrt3-\lambda_4}{(1/\sqrt3-\lambda_4)^3} - \frac{(3-\lambda_4)}{(1-\lambda_4)^3} \right]\tfrac{1}{6}E \right\} dy'. \quad (4.13)$$

We now have seven simultaneous equations in seven unknowns.

Solving the set of linear equations (4.6)–(4.11) for B, D, E, C_1, C_2, and C_3 as functions of y and $A(y)$, then substituting the results into (4.13) and collecting terms, we obtain

$$\left[\zeta_0 - 4\zeta_2 y + \frac{(\zeta_1+4\zeta_2+\tfrac{1}{4}\zeta_0)y}{(1-\tfrac{1}{4}y)} \right] yA(y) + \int_0^y \left[1 - \zeta_0 + 4\zeta_2 y' - \frac{(\zeta_1+4\zeta_2+\tfrac{1}{4}\zeta_0)y'}{(1-\tfrac{1}{4}y')} \right] A(y')dy'$$

$$= -4\ln(1-\tfrac{1}{4}y) + \frac{T_1 y^2}{(1-\tfrac{1}{4}y)} + \frac{\tfrac{1}{2}(T_2-\tfrac{1}{4}T_1)y^3}{(1-\tfrac{1}{4}y)^2} + \frac{\tfrac{1}{2}W_3 y^3(1+\tfrac{3}{4}y)}{(1-\tfrac{1}{4}y)^3} + \frac{(\tfrac{1}{3}W_4-\tfrac{1}{8}W_3)y^4(1+\tfrac{1}{4}y)}{(1-\tfrac{1}{4}y)^4}$$

$$- \int_0^y \left[\frac{T_1 y'}{(1-\tfrac{1}{4}y')} + \frac{\tfrac{1}{2}(T_2-\tfrac{1}{4}T_1)y'^2}{(1-\tfrac{1}{4}y')^2} + \frac{\tfrac{1}{2}W_3 y'^2(1+\tfrac{3}{4}y')}{(1-\tfrac{1}{4}y')^3} + \frac{(\tfrac{1}{3}W_4-\tfrac{1}{8}W_3)y'^3(1+\tfrac{1}{4}y')}{(1-\tfrac{1}{4}y')^4} \right] dy', \quad (4.14)$$

where the ζ's, T's, and W's depend only on λ_3 and λ_4. (Their quite complicated functional dependences on the parameters λ_3 and λ_4 are given in Appendix D.) Differentiating both sides of (4.14) with respect to y then yields

$$\left[\zeta_0 - 4\zeta_2 y + \frac{(\zeta_1+4\zeta_2+\tfrac{1}{4}\zeta_0)y}{(1-\tfrac{1}{4}y)} \right] y\frac{dA}{dy} + \left[1 - 4\zeta_2 y + \frac{(\zeta_1+4\zeta_2+\tfrac{1}{4}\zeta_0)y}{(1-\tfrac{1}{4}y)} + \frac{(\zeta_1+4\zeta_2+\tfrac{1}{4}\zeta_0)y^2}{(1-\tfrac{1}{4}y)^2} \right] A(y)$$

$$= \frac{1+T_1 y}{(1-\tfrac{1}{4}y)} + \frac{T_2 y^2}{(1-\tfrac{1}{4}y)^2} + \frac{(W_3+T_3 y)y^2}{(1-\tfrac{1}{4}y)^3} + \frac{(W_4+T_4 y)y^3}{(1-\tfrac{1}{4}y)^4} + \frac{(\tfrac{1}{3}W_4-\tfrac{1}{8}W_3)y^4(1+\tfrac{1}{4}y)}{(1-\tfrac{1}{4}y)^5}, \quad (4.15)$$

or after a certain amount of rearrangement,

$$\frac{dA}{dy} + \left\{ (\zeta_0 y)^{-1} + \tfrac{1}{4}(1-\tfrac{1}{4}y)^{-1} + \frac{\zeta_1(1-\zeta_0^{-1})-\tfrac{1}{4}+\zeta_2(2-\zeta_0^{-1})y}{\zeta_0+\zeta_1 y+\zeta_2 y^2} \right\} A(y)$$

$$= (\zeta_0+\zeta_1 y+\zeta_2 y^2)^{-1} \left\{ y^{-1} + T_1 + \frac{T_2 y}{(1-\tfrac{1}{4}y)} + \frac{(W_3+T_3 y)y}{(1-\tfrac{1}{4}y)^2} + \frac{(W_4+T_4 y)y^2}{(1-\tfrac{1}{4}y)^3} + \frac{(\tfrac{1}{3}W_4-\tfrac{1}{8}W_3)y^3(1+\tfrac{1}{4}y)}{(1-\tfrac{1}{4}y)^4} \right\}. \quad (4.16)$$

Moreover, it can easily be determined from (4.14) that

$$A(0) = 1. \quad (4.17)$$

Thus the integral equation (4.14) is equivalent to the linear first-order differential equation (4.16) together with the boundary condition (4.17).

When ζ_0 is positive, the solution to (4.16)–(4.17) can be written

$$A(y) = \frac{(1-\tfrac{1}{4}y)[\zeta_0+\zeta_1 y+\zeta_2 y^2]^{[(1/2\zeta_0)-1]}}{y^{1/\zeta_0}[(q+\zeta_1+2\zeta_2 y)/(q-\zeta_1-2\zeta_2 y)]^r} \int_0^y \frac{y'^{[(1/\zeta_0)-1]}}{[\zeta_0+\zeta_1 y'+\zeta_2 y'^2]^{1/2\zeta_0}} \left(\frac{q+\zeta_1+2\zeta_2 y'}{q-\zeta_1-2\zeta_2 y'} \right)^r \left[\frac{1+T_1 y'}{(1-\tfrac{1}{4}y')} + \frac{T_2 y'^2}{(1-\tfrac{1}{4}y')^2} \right.$$

$$\left. + \frac{(W_3+T_3 y')y'^2}{(1-\tfrac{1}{4}y')^3} + \frac{(W_4+T_4 y')y'^3}{(1-\tfrac{1}{4}y')^4} + \frac{(\tfrac{1}{3}W_4-\tfrac{1}{8}W_3)(1+\tfrac{1}{4}y')y'^4}{(1-\tfrac{1}{4}y')^5} \right] dy' \qquad r = \frac{2(\zeta_1/\zeta_0)+1}{4q}, \quad (4.18)$$

if the quantity

$$q^2 = \zeta_1^2 - 4\zeta_0\zeta_2 \quad (4.19)$$

is positive[25] or

$$A(y) = \frac{(1-y/4)[\zeta_0+\zeta_1 y+\zeta_2 y^2]^{[(1/2\zeta_0)-1]}}{y^{1/\zeta_0} \exp\{-[2(\zeta_1/\zeta_0)+1](2q^*)^{-1}\tan^{-1}[(\zeta_1+2\zeta_2 y)/q^*]\}} \int_0^y \frac{y'^{[(1/\zeta_0)-1]}}{[\zeta_0+\zeta_1 y'+\zeta_2 y'^2]} (2\zeta_0)^{-1}$$

$$\times \exp\left[\frac{[2(\zeta_1/\zeta_0)+1]}{2q^*}\tan^{-1}\left(\frac{\zeta_1+\zeta_2 y'}{q^*}\right)\right]\left[\frac{1+T_1 y'}{(1-\frac{1}{4}y')} + \frac{T_2 y'^2}{(1-\frac{1}{4}y')^2} + \frac{(W_3+T_3 y')y'^2}{(1-\frac{1}{4}y')^3} + \frac{(W_4+T_4 y')y'^3}{(1-\frac{1}{4}y')^4}\right.$$

$$\left.+ \frac{(\frac{1}{3}W_4-\frac{1}{8}W_3)(1+\frac{1}{4}y')y'^4}{(1-\frac{1}{4}y')^5}\right] dy' \qquad q^* = (4\zeta_0\zeta_2-\zeta_1^2)^{1/2}, \quad (4.20)$$

if q^2 is negative. On the other hand, when ζ_0 is negative (we shall not consider the special case $\zeta_0=0$), there are an infinite number of solutions to (4.16) which also satisfy (4.17). The general expressions are[26]

$$A(y) = \frac{(1-\frac{1}{4}y)y^{-1/\zeta_0}}{(-\zeta_0-\zeta_1 y-\zeta_2 y^2)^{(1-1/2\zeta_0)}} \left\{\frac{\zeta_1+q^*+2\zeta_2 y}{\zeta_1-q^*+2\zeta_2 y}\right\}^{-r} \int \frac{(-\zeta_0-\zeta_1 y-\zeta_2 y^2)^{-1/2\zeta_0}}{y^{(1-1/\zeta_0)}}\left(\frac{\zeta_1-q^*+2\zeta_2 y}{\zeta_1+q^*+2\zeta_2 y}\right)^{-r}$$

$$\times \left[\frac{1+T_1 y}{(1-\frac{1}{4}y)} + \frac{T_2 y^2}{(1-\frac{1}{4}y)^2} + \frac{(W_3+T_3 y)y^2}{(1-\frac{1}{4}y)^3} + \frac{(W_4+T_4 y)y^3}{(1-\frac{1}{4}y)^4} + \frac{(\frac{1}{3}W_4-\frac{1}{8}W_3)(1+\frac{1}{4}y)y^4}{(1-\frac{1}{4}y)^5}\right] dy \qquad q^2>0,^{25} \quad (4.21)$$

and

$$A(y) = \frac{(1-\frac{1}{4}y)y^{-1/\zeta_0}}{(-\zeta_0-\zeta_1 y-\zeta_2 y^2)^{[1-(1/2\zeta_0)]}} \exp\left[\frac{[2(\zeta_1/\zeta_0)+1]}{2q^*}\tan^{-1}\left(\frac{-\zeta_1+2\zeta_2 y}{q^*}\right)\right]\int \frac{(-\zeta_0-\zeta_1 y-\zeta_2 y^2)^{-1/2\zeta_0}}{y^{(1-1/\zeta_0)}}$$

$$\times \exp\left[\frac{-[2(\zeta_1/\zeta_0)+1]}{2q^*}\tan^{-1}\left(\frac{\zeta_1+2\zeta_2 y}{q^*}\right)\right]\left[\frac{1+T_1 y}{(1-\frac{1}{4}y)} + \frac{T_2 y^2}{(1-\frac{1}{4}y)^2} + \frac{(W_3+T_3 y)y^2}{(1-\frac{1}{4}y)^3} + \frac{(W_4+T_4 y)y^3}{(1-\frac{1}{4}y)^4}\right.$$

$$\left.+ \frac{(\frac{1}{3}W_4-\frac{1}{8}W_3)(1+\frac{1}{4}y)y^4}{(1-\frac{1}{4}y)^5}\right] dy \qquad q^2<0. \quad (4.22)$$

The only physically reasonable solution, however, is that for which $A(y)$ is analytic at $y=0$—a necessary condition if a virial series for $p/\rho kT$ is to exist.

The coefficients b_n in the virial series

$$p/\rho kT = A(y) = 1+b_2 y+b_3 y^2+b_4 y^3+\cdots+b_n y^{n-1}+\cdots \qquad (4.23)$$

can be determined from (4.18), (4.20), (4.21), or (4.22). It is more convenient, however, to substitute (4.23) and the corresponding expression for dA/dy directly into (4.16) and equate the coefficients of like powers of y on both sides of the resulting equation. In this manner, it is found that

$$b_2 = \tfrac{1}{2}, \qquad (4.24)$$

$$b_3 = (T_2+W_3-\tfrac{3}{16}\zeta_0-\tfrac{5}{4}\zeta_1-2\zeta_2+\tfrac{1}{8})/(1+2\zeta_0), \qquad (4.25)$$

$$b_4 = \left[T_3+W_4+\left(\frac{1}{4}-\frac{\zeta_1}{\zeta_0}\right)T_2+\left(\frac{1}{2}-\frac{\zeta_1}{\zeta_0}\right)W_3-(\zeta_1+\tfrac{1}{4}\zeta_0)(1-\zeta_0^{-1})b_3+\frac{5}{4}\frac{\zeta_1^2}{\zeta_0}-\tfrac{7}{4}\zeta_2-\tfrac{3}{64}\zeta_0-\frac{\zeta_1}{8\zeta_0}+\frac{2\zeta_1\zeta_2}{\zeta_0}\right](1+3\zeta_0)^{-1},$$

$$(4.26)$$

with more complicated expressions for b_5, b_6, etc.

From (4.18), (4.20), (4.21), or (4.22), the function $A(y)$ can be constructed for an arbitrary pair (λ_3, λ_4). Then the remaining "coefficients" needed to determine $G(\lambda, y)$ can be obtained by substituting A back into the expressions for B, D, E, C_1, C_2, and C_3 [as functions of y and $A(y)$] derived from the set of linear equations (4.6)–(4.11).

V. RESULTS

The function $A(y)$ must be constructed numerically since the integrals in (4.18)–(4.22) cannot be expressed in terms of elementary functions. Equations (4.18) and (4.20) can be employed directly to evaluate A, but

(4.21) and (4.22) are of little practical utility because of the presence of the indefinite integrals. For $\zeta_0<0$, therefore, the equation of state has been determined by solving the differential equation (4.16) numerically, using the fourth-order Runge–Kutta procedure.[27] As is apparent from (4.21) and (4.22), specifying that $A(0)=1$ and $(dA/dy)_{y=0}=\frac{1}{2}$ is sufficient to single out that solution for which A is analytic at $y=0$ only when $\zeta_0\leq-1$. Consequently, when $-1<\zeta_0<0$, the Runge–Kutta "machinery" must be started at some $y\neq0$. In such cases, $y=0.01$ has been used as the initial value, since $A(0.01)$ can be determined to 11 significant figures from the virial series (4.24) truncated after

TABLE I. The branch points y_+ and y_- for a number of pairs (λ_3, λ_4).

λ_3	λ_4	y_+	y_-
0	0	-1.825	5.515
0	0.2	0.546	5.247
0	0.4	1.973	4.939
0	0.55	2.734	4.669
0.1	0	27.906	6.332
0.2	0	1.479	5.088
0.2	0.09	3.800	4.087
0.2	0.1	$4.288-1.149i$	$4.288+1.149i$
0.2	0.12	-450.676	6.053
0.2	0.14	-0.561	5.388
0.2	0.2	1.365	5.111
0.2	0.4	2.603	4.771
0.2	0.55	3.139	4.534
0.4	0	2.261	4.880
0.4	0.2	2.813	4.703
0.4	0.34	3.557	4.330
0.4	0.35	$4.056-0.517i$	$4.056+0.517i$
0.4	0.36	-1.769	5.394
0.4	0.4	3.088	4.589
0.4	0.55	3.510	4.360
0.55	0	2.991	4.591
0.55	0.2	3.298	4.469
0.55	0.4	3.591	4.314
0.55	0.544	$4.126-0.600i$	$4.126+0.600i$
0.55	0.55	3.774	4.190

$b_5 y^4$, yet 0.01 is large enough so that the terms $A/\zeta_0 y$ and $[y(\zeta_0+\zeta_1 y+\zeta_2 y^2)]^{-1}$ cause no serious loss of significant figures during the initial stages of the iterative computations. When $\zeta_0 > 0$, on the other hand, $A(y)$ has been calculated from (4.18) or (4.20), using Simpson's rule to evaluate the integrals. Before presenting the results, let us examine briefly the analytic structure of the function $A(y)$.

It is apparent from (4.18)–(4.22) that $A(y)$ has a pole of order 3 at $y=4$. When ζ_0 is irrational [as is the case for all pairs (λ_3, λ_4) with which we shall be concerned], it also has branch points of infinite order at the roots

$$y_\pm = [-\zeta_1 \pm (\zeta_1^2 - 4\zeta_0\zeta_2)^{1/2}]/2\zeta_2 \qquad (5.1)$$

of the quadratic equation

$$\zeta_0 + \zeta_1 y + \zeta_2 y^2 = 0. \qquad (5.2)$$

These branch points have been located for approximately 400 carefully selected pairs (λ_3, λ_4) and a sampling of the results is given in Table I. For all pairs (λ_3, λ_4) such that $0 \leq \lambda_3 < 1/\sqrt{3}$ and $0 \leq \lambda_4 < 1/\sqrt{3}$ (excluding those pairs for which any of ζ_0, ζ_1, ζ_2, or the discriminant q^2 vanishes), y_+ and y_- are described by one of the following: (I) Both y_+ and y_- are complex with real parts >4. (II) Both y_+ and y_- are real with $y_+ < 0$ and $y_- > 4$. (III) Both y_+ and y_- are real with $0 < y_+ < 4$ and $y_- > 4$. (IV) Both y_+ and y_- are real and > 4.

Which of these statements is correct for a specific (λ_3, λ_4) can be seen from Fig. 5, where the $\lambda_3\lambda_4$ plane is divided into four regions, each labeled with the appropriate Roman numeral (i.e., at points in region I, statement I is true, etc.)

Neither the complex branch points nor the real ones greater than 4 need concern us, since $y > 4$ is physically meaningless. (To be precise, $y > 2\pi/\sqrt{3} \approx 3.63$ is unattainable since $2\pi/\sqrt{3}$ is the density y_0 at close packing.) Likewise, a root $y_+ < 0$ does not interfere with the calculation of $A(y)$ using (4.18) ($y_+ < 0$ corresponds to $\zeta_0 > 0$, $q^2 > 0$.), although the virial expansion (4.23) will not converge for $y > -y_+$ in such cases. We need, however, to look more clearly at points (λ_3, λ_4) in region III. There the equation of state is formally given by (4.21) since $0 < y_+ < 4$ corresponds to $\zeta_0 < 0$, $q^2 > 0$, and $|\zeta_1/q^*| > 1$. Let us, however, use the alternative expression[28]

$$A(y) = \frac{(1-\tfrac{1}{4}y)y^{-1/\zeta_0}}{(y_+-y)^{(p_1+1)}(y_--y)^{(p_2+1)}}$$

$$\times \left\{ \int_{y_l}^y \frac{(y_+-y')^{p_1}(y_--y')^{p_2}}{\zeta_2 y'^{(1-1/\zeta_0)}} \left[\frac{1+T_1 y'}{(1-\tfrac{1}{4}y')} + \frac{T_2 y'^2}{(1-\tfrac{1}{4}y')^2} \right. \right.$$

$$+ \frac{(W_3+T_3 y')y'^2}{(1-\tfrac{1}{4}y')^3} + \frac{(W_4+T_4 y')y'^3}{(1-\tfrac{1}{4}y')^4}$$

$$\left. \left. + \frac{(\tfrac{1}{3}W_4 - \tfrac{1}{8}W_3)(1+\tfrac{1}{4}y')y'^4}{(1-\tfrac{1}{4}y')^5} \right] dy' + C_l \right\}, \quad (5.3)$$

$$\equiv F_1(y) \left[\int_{y_l}^y F_2(y') dy' + C_l \right], \qquad (5.4)$$
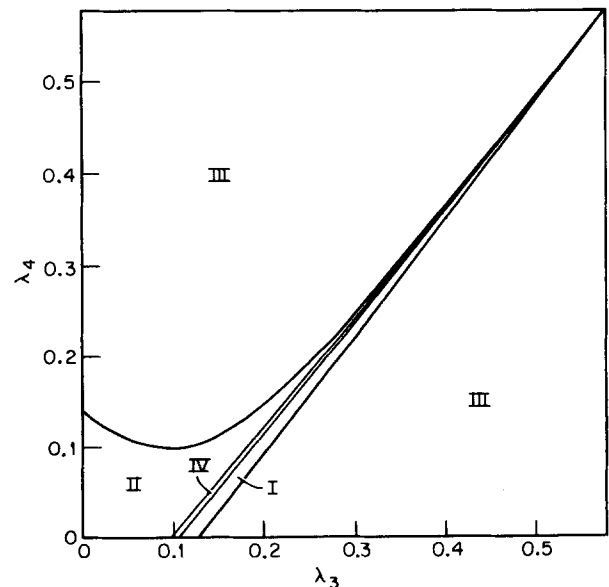

FIG. 5. Regions in the $\lambda_3\lambda_4$ plane. At points (λ_3, λ_4) in region I, the branch points y_+ and y_- are both complex. In regions II, III, and IV, respectively, $y_+ < 0$, $y_- > 4$; $0 < y_\pm < 4$; and $y_\pm > 4$.

where

$$p_1 = -(2\zeta_0)^{-1} - \frac{[2(\zeta_1/\zeta_0)+1]}{4q},$$

$$p_2 = -(2\zeta_0)^{-1} + \frac{[2(\zeta_1/\zeta_0)+1]}{4q}, \quad (5.5)$$

y_l is some fixed lower limit ($\neq 0$), and C_l is a constant chosen so that[28]

$$C_l F_1(y_l) = A(y_l). \quad (5.6)$$

Since F_2 vanishes when $y' = y_+$, the integral is finite when $y = y_+$, and it follows that $A(y)$ diverges as $1/(y_+ - y)^{(p_1+1)}$ as $y \to y_+$. Moreover, it can be shown that A is complex valued for $y_+ < y < 4$. Clearly, therefore, we cannot use any pair of parameters (λ_3, λ_4) for which y_+ occurs at a low or moderate density. The exponent (p_1+1) is very large when y_+ is close to zero (since $y_+ \to 0$ as $\zeta_0 \to 0$), but decreases as y_+ increases. For y_+ in the vicinity of $y_0 = 2\pi/\sqrt{3}$, $p_1+1 \approx 1.9$. [In contrast to this the exact function $p/\rho kT(y)$ is believed to diverge as $(1-y/y_0)^{-1}$ as $y \to y_0$.[29]]

$A(y)$ has been calculated—at intervals $\Delta y = 0.02$—from $y = 0$ to $y = 4$ (or to $y = y_+$, where appropriate) at 26 carefully selected points in the $\lambda_3 \lambda_4$ plane: 15 from
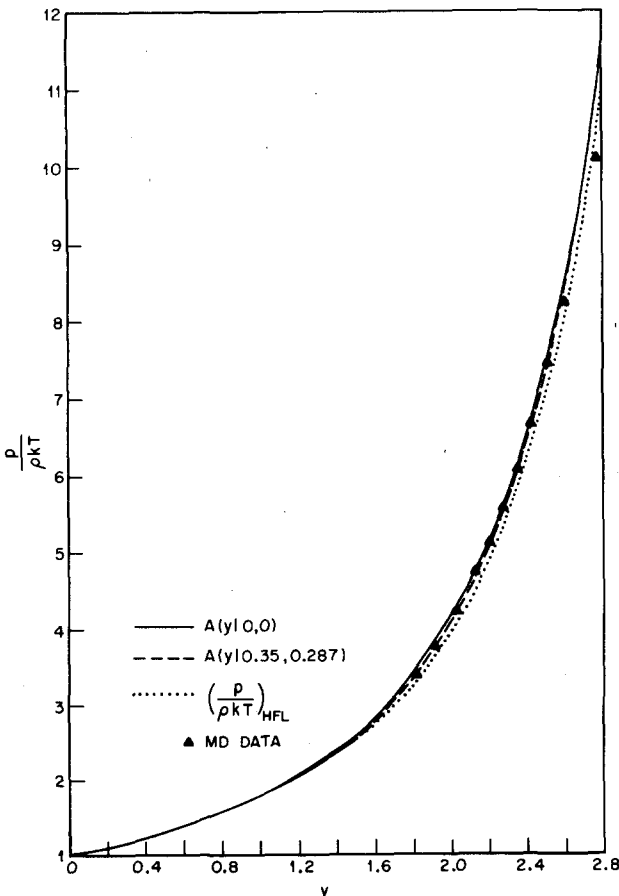

FIG. 6. A comparison of three theoretical equations of state with the molecular dynamics results of Alder and Wainwright.[30,31]
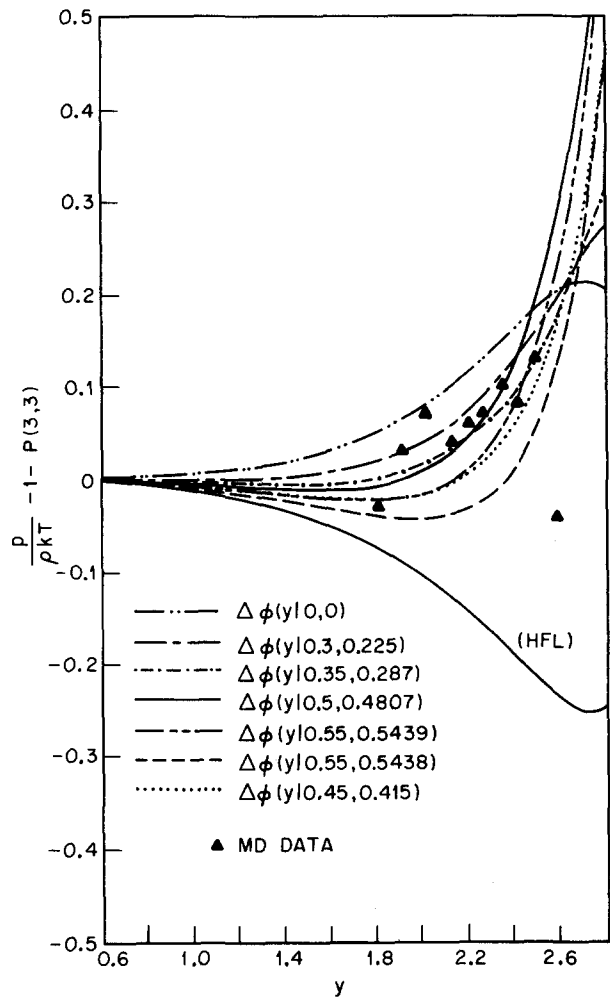

FIG. 7. The quantity $\Delta\phi = p/\rho kT - 1 - P(3, 3)$ from the molecular dynamics data of Alder and Wainwright,[30,31] from HFL theory, and from extended scaled particle theory with seven different pairs (λ_3, λ_4). $P(3, 3)$ is the Ree and Hoover Padé approximant[33] given by Eq. (5.7).

region I (here small changes in λ_3 or λ_4 produce relatively large changes in the equation of state), 4 from region II, 5 from region III, and 2 from region IV. On the basis of this "sampling," plus a knowledge of y_+, y_-, and the virial coefficients b_3, b_4, and b_5 for approximately 400 pairs (λ_3, λ_4), we are confident that the dependence of $A(y)$ on λ_3 and λ_4 is well understood, qualitatively. [The qualitative behavior of $A(y)$ can rather accurately be predicted from the values of the virial coefficients and the locations of the branch points.]

In Fig. 6, $p/\rho kT = A(y)$ from $y = 0$ to $y = 2.80$ for two sets of parameters (λ_3, λ_4): $(0, 0)$ and $(0.35, 0.287)$, are compared with the HFL equation of state and with the rigid disk molecular dynamics (MD) results of Alder and Wainwright.[30,31] Except at the highest densities shown, it is clear that the MD triangles lie slightly below the $(0, 0)$ curve and somewhat above the HFL curve, but can be fitted quite well with the $(0.35, 0.287)$ curve. The first ten triangles represent a 72 disk system,
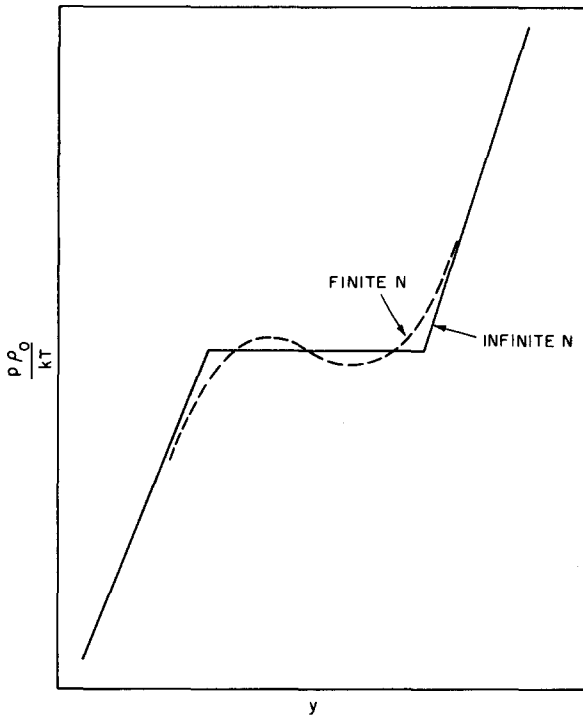
FIG. 8. The dimensionless pressure $p p_0/kT$ as a function of dimensionless density y near the "freezing" transition for rigid disks. The solid curve is characteristic of a first-order transition in an infinite system, while the dashed curve is an hypothetical isotherm for a finite system with N of order 10^2-10^3.

while the last triangle, at $y = 2.765$, represents a periodic assembly of 870 hard disks. The latter undergoes a transition from a fluid with $y \approx 2.765$ to a "solid" with $y \approx 2.865$, and this result leaves very little doubt that an infinite system of rigid disks also exhibits a "freezing" transition, although probably with somewhat different "coexisting" densities. Unfortunately, we have not observed such a transition at any density for any pair (λ_3, λ_4). Rather, $A(y)$ monotonically increases from $y = 0$ to $y = y_m$, where $y_m \geq 3.6$, for all (λ_3, λ_4) which lead to acceptable equations of state over the fluid range of densities.[32] Thus, our extended scaled particle theory has failed to achieve one of its prime goals, even though it can provide a very good description of the rigid disk fluid, at least for $y \leq 2.50$. (The positions of the last two MD points relative to the theoretical curves will be discussed somewhat later.)

Figure 7 presents a comparison of the molecular dynamics results, the HFL equation of state, and the functions $p/\rho kT$ for (λ_3, λ_4) equal to $(0, 0)$, $(0.3, 0.225)$, $(0.35, 0.287)$, $(0.45, 0.415)$, $(0.5, 0.4807)$, $(0.55, 0.5439)$, and $(0.55, 0.5438)$, respectively. Instead of $p/\rho kT$ itself, the difference $\Delta\phi \equiv (p/\rho kT) - 1 - P(3, 3)$ is plotted, where $P(3, 3)$ is the Ree and Hoover Padé approximant[33] to $p/\rho kT - 1$ for rigid disks, given by

$$P(3, 3) = \frac{\frac{1}{2}y - 0.0505200y^2 + 0.0006986y^3}{1 - 0.492043y + 0.0607290y^2}. \quad (5.7)$$

This use of $P(3, 3)$ as a "base line" makes it possible to

display quite clearly—and in considerable detail—differences among the theoretical curves as well as discrepancies between theory and "experiment." Of the seven pairs (λ_3, λ_4) represented, six correspond to points in region I of the $\lambda_3\lambda_4$ plane of Fig. 5. This reflects the fact that the best equations of state are obtained in this region, if we define a "good" equation of state to be one that fits the molecular dynamics data well. In regions II and IV, the curves $\Delta\phi(y | \lambda_3, \lambda_4)$[34]—and, therefore, $A(y | \lambda_3, \lambda_4)$[34]—for all (λ_3, λ_4) lie significantly above the MD points, while in region III, the equations of state range from quite poor to highly pathological, except where the branch point $y_+ \to 4$. (This occurs very near the lower boundary of region I and in a very small area with $\lambda_3 > 0.5$ and $\lambda_4 \to 1/\sqrt{3}$.) In particular, when y_+ is near the close packed density $y_0 = 2\pi/\sqrt{3}$, $A(y | \lambda_3, \lambda_4)$ lies far below the MD results. $\Delta\phi(y | 0, 0)$—the "best" curve from regions II and IV—is included to facilitate comparisons with Fig. 6.

The curves $\Delta\phi(y | 0.3, 0.225)$, $\Delta\phi(y | 0.35, 0.287)$, $\Delta\phi(y | 0.45, 0.415)$, and $\Delta\phi(y | 0.55, 0.5438)$ in Fig. 7 indicate clearly how the function $A(y | \lambda_3, \lambda_4)$ changes as the point (λ_3, λ_4) moves along the lower boundary of region I toward $(1/\sqrt{3}, 1/\sqrt{3})$; namely, if (λ_3', λ_4') and $(\lambda_3'', \lambda_4'')$ are two points on such a path, with the latter closer to $(1/\sqrt{3}, 1/\sqrt{3})$, then

$$A(y | \lambda_3'', \lambda_4'') < A(y | \lambda_3', \lambda_4') \qquad y < Y,$$

$$A(y | \lambda_3'', \lambda_4'') > A(y | \lambda_3', \lambda_4') \qquad y > Y,$$

where Y, the intersection of the curves $A(y | \lambda_3', \lambda_4')$ and $A(y | \lambda_3'', \lambda_4'')$, increases with the distance between (λ_3', λ_4') and $(\lambda_3'', \lambda_4'')$. The same sort of behavior occurs as (λ_3, λ_4) moves toward $(1/\sqrt{3}, 1/\sqrt{3})$ along the upper boundary or through the center [compare $\Delta\phi(y | 0.5, 0.4807)$ and $\Delta\phi(y | 0.55, 0.5439)$] of region I, or through region IV, or through the "thin" part of region II. [$A(y | \lambda_3, \lambda_4)$ changes little throughout the "fat" part of region II near the origin.] On the other hand, as (λ_3, λ_4) crosses region I from the lower to the upper boundary, each succeeding curve $A(y | \lambda_3, \lambda_4)$ lies above its predecessor at all densities, with small changes in (λ_3, λ_4) producing relatively large changes in the equation of state. [Compare $\Delta\phi(y | 0.55, 0.5438)$ and $\Delta\phi(y | 0.55, 0.5439)$.]

The statistical uncertainty in the molecular dynamics data can be estimated from their scatter in Fig. 7, since $\Delta\phi_{MD}$ must be a smoothly varying function of y at all densities below the transition. Within the estimated uncertainty, it is clear that at least $\Delta\phi(y | 0.35, 0.287)$ and $\Delta\phi(y | 0.5, 0.4807)$ fit the first nine MD triangles. However, how are we to interpret the large deviations of the theoretical curves from the last two triangles, at $y = 2.59$ ($\Delta\phi = -0.04$) and $y = 2.765$ ($\Delta\phi = -0.61$), respectively? There are two relevant possibilities: (1) The 72/870 disk MD results adequately represent an infinite hard disk system arbitrarily close to the "freezing" transition, in which case our theory

provides a rather poor description of the rigid disk fluid over the highest 10% of its density range, despite the excellent agreement with "experiment" at lower densities. (2) The 72/870 disk results do not accurately describe the infinite system near the transition; rather, the rapid decrease in $\Delta\phi_{\mathrm{MD}}(y)$ as the transition is approached represents a kind of premonitory phenomenon resulting directly from the small numbers of disks considered. In this case, our theory may be able to describe the rigid disk fluid well at all densities. It is clear that both the 72 and 870 disk assemblies exhibit significant finite-size effects, since the former fluctuates between a high-pressure fluid state and a low-pressure "solid" state between $y\approx2.69$ and $y\approx2.73$, while the latter yields an isotherm $\beta p(y)$ with a van der Waals type loop between $y\approx2.765$ and $y\approx2.865$. However, there is at present no compelling reason to expect that a small system should display a premonitory flattening of $\beta p(y)$ as the transition is approached. Nevertheless, this is not an unreasonable suggestion, as is indicated by Fig. 8, which compares a p–y isotherm for an infinite system (solid curve), with an hypothetical finite system approximation to it (dashed curve). (Note that the singularities at the solid and fluid densities have been rounded off in such a way that the pressure in the finite system is too low below the transition and too high above it.) Whatever the merits of this conjecture, it appears that the molecular dynamics computations have not conclusively determined the behavior of the rigid disk system near the transition, in the thermodynamic limit. (This would seem to require considerably more than 870 disks.) Therefore, we shall assess the functions $A(y\mid\lambda_3,\lambda_4)$ strictly on the basis of their agreement with the first nine MD triangles (for which $y<2.50$) and shall regard their usefulness at higher densities as an open question.

One measure of the agreement between any theoretical equation of state $p/\rho kT=\phi(y)$ and the molecular dynamics results is the average percent deviation ϵ, defined by

$$\epsilon=100\sum_{i=1}^{9}\left|\frac{\phi(y_i)-\phi_{\mathrm{MD}}(y_i)}{\phi_{\mathrm{MD}}(y_i)}\right|, \qquad (5.8)$$

TABLE II. Percent deviations from the molecular dynamics data and from the exact virial coefficients b_3, b_4, and b_5.

(λ_3,λ_4)	ϵ	Δb_3	Δb_4	Δb_5
(0, 0)	1.1	0.39	4.36	7.16
(0.3, 0.225)	0.8	−1.35	0.35	3.58
(0.35, 0.287)	0.5	−2.18	−1.32	1.44
(0.45, 0.415)	0.9	−3.18	−3.28	−1.11
(0.5, 0.4807)	0.6	−2.97	−2.54	0.30
(0.55, 0.5438)	1.5	−3.76	−4.54	−2.94
(0.55, 0.5439)	0.8	−3.42	−3.61	−1.35
HFL	4.8	−4.09	−6.13	−6.38
Padé	1.2	...	...	...

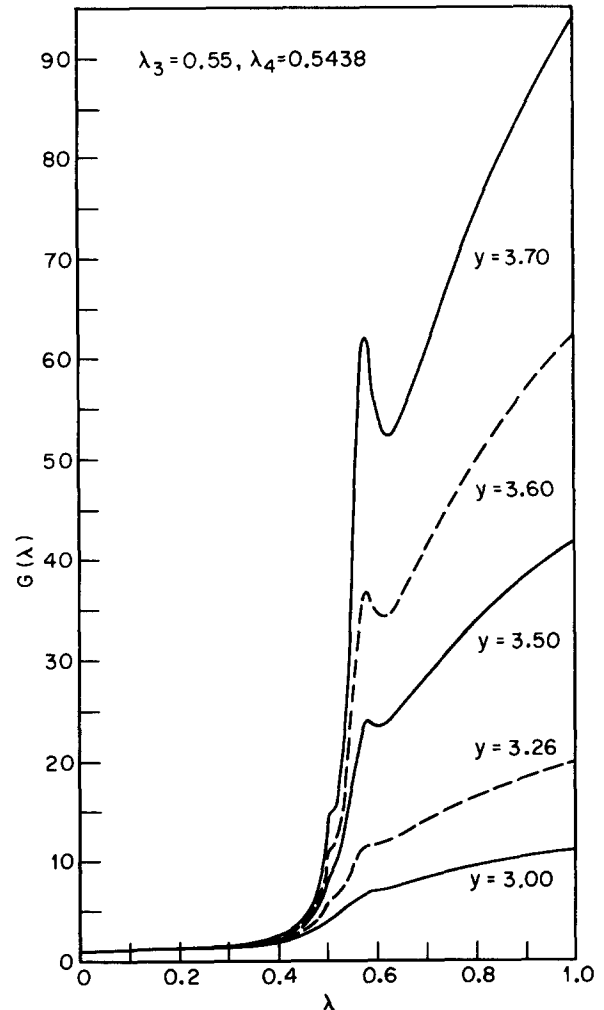FIG. 9. The contact pair correlation function $G(\lambda)$ at five fixed values of y. $\lambda_3=0.55$, $\lambda_4=0.5438$.

where the sum is over the nine MD points with $y\le2.50$. Table II lists the values of ϵ for the nine functions $p/\rho kT$ represented in Fig. 7. The curves $A(y\mid0.3,0.225)$, $A(y\mid0.35,0.287)$, $A(y\mid0.45,0.415)$, $A(y\mid0.5,0.4807)$, and $A(y\mid0.55,0.5439)$ all agree with ϕ_{MD} within 1%, the reported uncertainty in the machine computations.[30,31] (Note that, in contrast to this, $\epsilon_{\mathrm{HFL}}=4.8\%$.) Furthermore, the value of ϵ (0.5%) for $(\lambda_3,\lambda_4)=$ (0.35, 0.287) confirms what is apparent from Fig. 7: that $A(y\mid0.35,0.287)$ fits the MD data in an excellent manner. In fact, it provides a considerably better fit than does the Padé approximant $P(3,3)$, which was hitherto regarded as the best analytic approximation to the machine results. Finally, Table II also gives, for each equation of state, the percent deviation Δb_j of the virial coefficients b_3, b_4, and b_5 from their exact values $b_3=0.1955$, $b_4=0.06659\pm0.00006$, and $b_5=0.02086\pm 0.00003$.[35] Clearly, the best values of b_3 do not correspond to the best equations of state. Also, it is apparent that producing very accurate virial coefficients is not the forte of our theoretical apparatus.
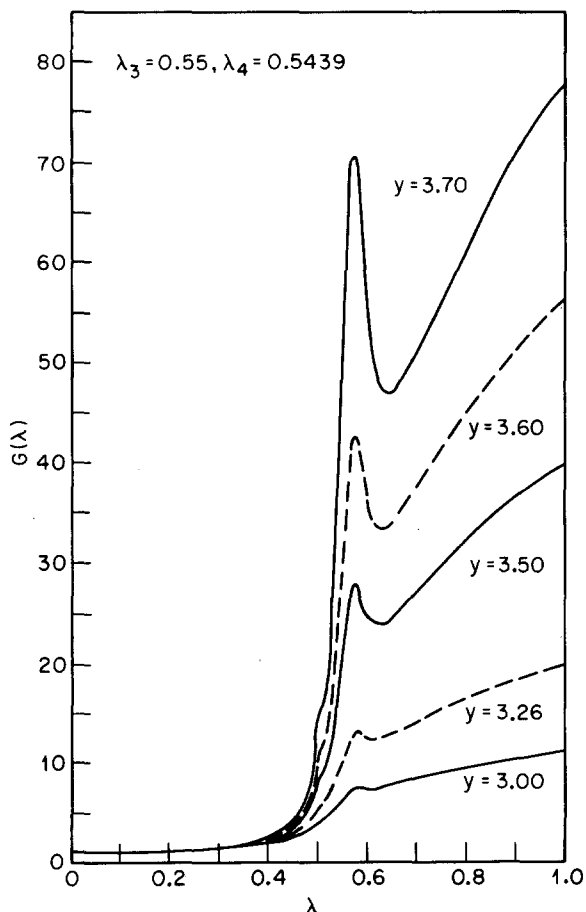
FIG. 10. The contact pair correlation function $G(\lambda)$ at five fixed values of y. $\lambda_3 = 0.55$, $\lambda_4 = 0.5439$.

For the remainder of this section, let us turn our attention to the contact pair correlation function G, given by (2.1), (4.1), and (4.4) when $\lambda < \frac{1}{2}$, $\frac{1}{2} \leq \lambda < 1/\sqrt{3}$, and $\lambda \geq 1/\sqrt{3}$, respectively. [As noted in Sec. IV, the coefficients B, D, E, C_1, C_2, and C_3 can be calculated at any fixed density $y = Y$ from (4.6) through (4.11) once $A(Y)$ has been evaluated.] In order to determine its behavior at high densities, we have evaluated $G(\lambda, y)$ from $\lambda = 0$ to $\lambda = 2$ for five to seven fixed values of y at each of 18 points in the $\lambda_3 \lambda_4$ plane of Fig. 5. Some results for four selected pairs (λ_3, λ_4) are shown in Figs. 9–12.

In Sec. II, it was argued that G should be a non-monotonic function of λ for the rigid disk "solid" and that, at sufficiently high densities, it should resemble $G(\lambda, \rho_0)$ (Fig. 3) with the spike near $\lambda = \frac{1}{2}$ rounded off and the divergences replaced by finite maxima. Despite its failure to predict a phase transition, our extended scaled particle theory can produce—for selected pairs (λ_3, λ_4)—functions $G(\lambda, y \mid \lambda_3, \lambda_4)$ with roughly the hoped for qualitative behavior over the range $0 \leq \lambda < 1$ at certain very high densities. This is demonstrated by Figs. 9 and 10, where $(\lambda_3, \lambda_4) = (0.55, 0.5438)$ and $(0.55, 0.5439)$, respectively. In both cases, at sufficiently

high densities, the curves $G(\lambda)$ exhibit a shoulder just above $\lambda = \frac{1}{2}$, then rise steeply and go through a maximum (just above $1/\sqrt{3}$) followed by a minimum, after which they rise monotonically up to $\lambda = 1$—a description that should also apply to the exact $G(\lambda, y)$. However, it is apparent that neither $G(\lambda \mid 0.55, 0.5438)$ nor $G(\lambda \mid 0.55, 0.5439)$ diverges at $\lambda = 1/\sqrt{3}$ or $\lambda = 1$ when $y = y_0 = 2\pi/\sqrt{3}$. Rather, both are everywhere smoothly varying functions of λ for all $y < 4$, at which density all the coefficients A, B, D, E, C_1, C_2, and C_3 diverge and a limit function $G(\lambda, y = 4)$ does not exist for $\lambda \geq \frac{1}{2}$. Moreover, for both pairs (λ_3, λ_4), the minima in $G(\lambda)$ somewhat above $1/\sqrt{3}$ are much too shallow; the slopes $\partial G/\partial \lambda$ are too small near $\lambda = 1$; and G remains a monotonic function of λ up to a density y', which seems to be considerably too high. Despite these deficiencies, both sets of curves are great improvements over those obtained from the HFL expression for $G(\lambda, y)$. (See Fig. 13.) Clearly, our extended theory represents a step in the right direction with regard to describing the rigid disk system at high densities.

Functions $G(\lambda, y)$ similar to those in Figs. 9–11 [i.e., with the same number of maxima and minima in $G(\lambda)$ at high densities, arranged in the same order] are obtained only in portions of region I of the $\lambda_3 \lambda_4$ plane. In regions II and IV and in the "usable"[36] parts of region III, the contact pair correlation functions qualitatively resemble $G(\lambda, y \mid 0, 0)$ (see Fig. 12); that is, for sufficiently large y, $G(\lambda)$ has a maximum at or slightly above $\lambda = \frac{1}{2}$, then a minimum somewhere
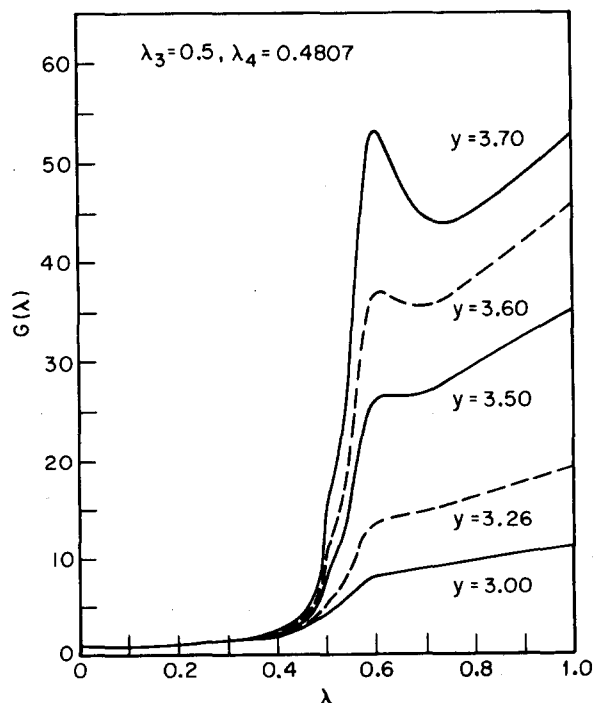

FIG. 11. The contact pair correlation function $G(\lambda)$ at five fixed values of y. $\lambda_3 = 0.5$, $\lambda_4 = 0.4807$.

beyond $\lambda = 1/\sqrt{3}$ (at which G may be negative), after which it monotonically increases, at least up to $\lambda = 2$. Within region I, $G(\lambda, y)$ changes with λ_3 and λ_4 in a fairly complicated manner. As the point (λ_3, λ_4) moves away from $(1/\sqrt{3}, 1/\sqrt{3})$ along a path near the center of the region, it can be seen, from Figs. 10 and 11, that (1) $G(\lambda)$ remains monotonic up to higher densities. (2) The shoulders near $\lambda = \frac{1}{2}$ become less pronounced. (3) The maxima occurring just above $\lambda = 1/\sqrt{3}$ slowly move to the right (i.e., to larger values of λ). (4) The minima following these maxima move more rapidly to the right, markedly broadening the "half peaks" between the two extrema. On the other hand, from Figs. 9 and 10, it is clear that if λ_3 is held constant and λ_4 increases so that (λ_3, λ_4) moves across region I from the lower to the upper boundary, the following changes in $G(\lambda, y)$ occur: (1) Nonmonotonicity in $G(\lambda)$ first appears at a lower density. (2) The shoulders near $\lambda = \frac{1}{2}$ again become less pronounced. (3) The positions λ_m of the maxima somewhat beyond $1/\sqrt{3}$ slowly move to the left while the quantities $G(\lambda_m)$ rapidly increase. The last trend continues until the $G(\lambda_m)$ diverge at some point (λ_3, λ_4'). (λ_4' appears to be independent of density as long as y is large enough so that $G(\lambda)$ is nonmonotonic.) For $\lambda_4 > \lambda_4'$, the functions $G(\lambda, y)$ qualitatively resemble $G(\lambda, y \mid 0, 0)$ (Fig. 12), and as $\lambda_4 \to \lambda_4'$ from above, the positions λ_m of the minima move to the right and $G(\lambda_m) \to -\infty$.

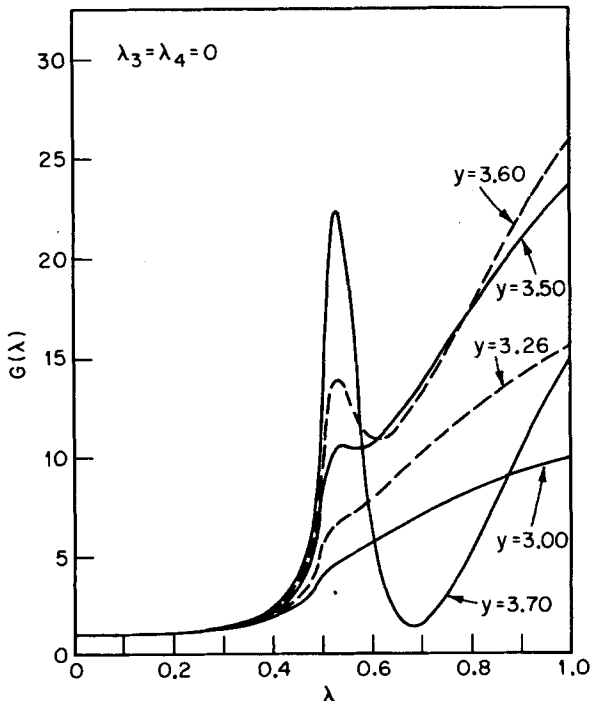From the figures, it is apparent that the best looking high density contact pair correlation functions are

FIG. 12. The contact pair correlation function $G(\lambda)$ at five fixed values of y. $\lambda_3 = \lambda_4 = 0$.
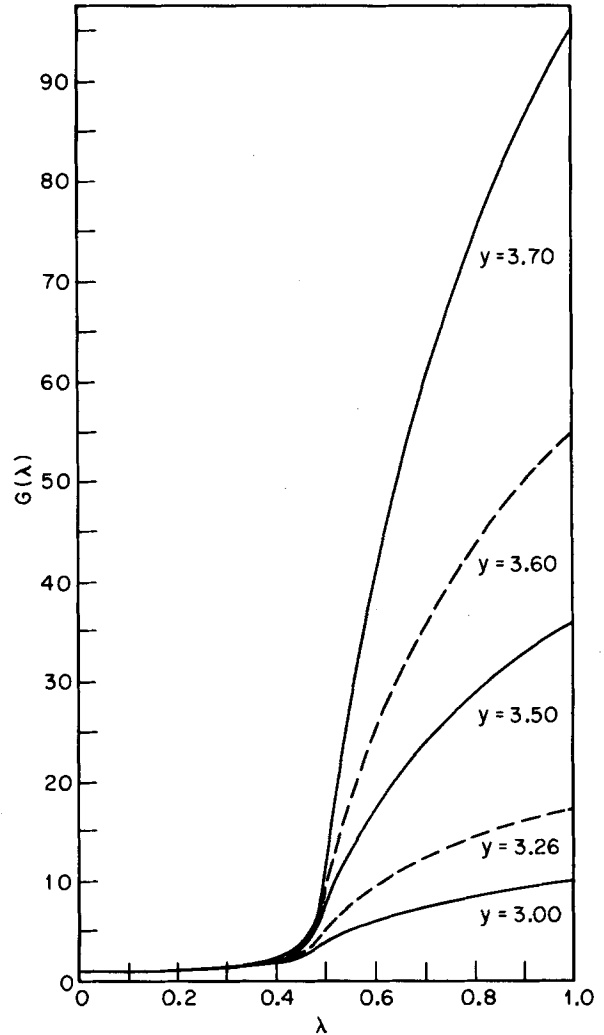

FIG. 13. The HFL contact pair correlation function $G(\lambda)$ at five fixed values of y.

obtained with (λ_3, λ_4) near $(1/\sqrt{3}, 1/\sqrt{3})$, where the equations of state are not particularly good. [See, for example, $\Delta\phi(y \mid 0.55, 0.5438)$ in Fig. 7.] On the other hand, while $A(y \mid 0.35, 0.287)$ proved to be our best equation of state, $G(\lambda, y \mid 0.35, 0.287)$ is not very appealing. Taking both $G(\lambda, y)$ and $A(y)$ into consideration, it appears that of all the pairs of parameters we have considered, the best results, on balance, can be obtained with (λ_3, λ_4) equal to $(0.5, 0.4807)$ or $(0.55, 0.5439)$.

In the interval $\frac{1}{2} \leq \lambda < 1/\sqrt{3}$, our theory seems to do a reasonably good job of predicting the λ dependence of the contact correlation function at certain high densities. [To see this illustrated, compare $G(\lambda, 3.60)$ for (λ_3, λ_4) equal to $(0.55, 0.5438)$ or $(0.55, 0.5439)$ with the exact $G(\lambda, y_0)$.] For fixed values of λ within this interval, it is less successful in predicting the y dependence of G. Certainly, it does not yield a good enough $C_1(y)$, since the equation of state gives no indication of

a phase transition. [Recall (4.10).] Moreover, at very low densities, the relations

$$a(\partial g^{(2)}/\partial r_{12})_{r_{12}=a}$$
$$= (3\pi/64y)\{5(1-\tfrac{1}{4}y)C_2+\tfrac{1}{2}[1-(57/4)y]C_1\}, \quad (5.9)$$

$$a^2(\partial^2 g^{(2)}/\partial r_{12}^2)_{r_{12}=a} = (3\pi/256y)\{35(1-\tfrac{1}{4}y)C_3$$
$$-(15/2)[1+(23/4)y]C_2$$
$$-(143/8)[1+(569/286)y+(14\ 451/4552)y^2]C_1\},$$
$$(5.10)$$

derived from the definitions of C_1, C_2, and C_3, give quite poor values for the slope and curvature of the radial distribution function $g^{(2)}(r_{12})$ at $r_{12}=a$. [Both these quantities should vanish as $y\rightarrow 0$. As obtained from (5.9) and (5.10), however, they are both finite at zero density.]

VI. DISCUSSION

The extended scaled particle theory just presented was directed toward describing the rigid disk system satisfactorily at high densities, a task which involves two closely related goals: (1) to produce functions $G(\lambda, y=y')$ with the proper shape when y' is large; (2) to predict the occurrence of a "freezing" transition. Although we have completely failed to achieve the latter goal, enough progress has been made toward the former to convince us that we are "on the right track." Therefore, it seems appropriate to discuss in some detail possible further extensions of the theory.

The first such extension which comes to mind utilizes the one exact condition on $G(\lambda, y)$ which has been derived but not used directly: the jump in $\partial^4 G/\partial\lambda^4$ at $\lambda=1/\sqrt{3}$, given by Eq. (C10) of Appendix C. In its present form, this expression cannot serve our purposes, since it introduces an additional unknown as well as providing another condition.[37] However, if the triple contact triplet correlation function $g^{(3)}(a, a, a, \rho)$ were replaced by its equivalent in the superposition approximation, $[g^{(2)}(a, \rho)]^3$ or $[G(1, y)]^3$, then (C10) would enable us to add a term proportional to $(\lambda-\tfrac{1}{2})^{9/2}$ to our expression for $G(\tfrac{1}{2}\leq\lambda<1/\sqrt{3})$ [the complete expansion of G about $\lambda=\tfrac{1}{2}$ also contains a term proportional to $(\lambda-\tfrac{1}{2})^4$, whose coefficient can be shown to equal $\tfrac{2}{5}yC_1^2$] or an additional term to $G(\lambda\geq 1/\sqrt{3})$ as given by (4.4). In either case, we could then derive eight simultaneous equations in eight unknowns: the analogues of (4.6)–(4.12), together with a new nonlinear relation obtained by adding the right-hand side of (C10) to

$$[\partial^4 G(\tfrac{1}{2}\leq\lambda<1/\sqrt{3})/\partial\lambda^4]_{\lambda=1/\sqrt{3}}$$

[from (4.1)] and equating the sum to

$$[\partial^4 G(\lambda\geq 1/\sqrt{3})/\partial\lambda^4]_{\lambda=1/\sqrt{3}}$$

[from (4.4)]. Such a system of equations would, in principle, be only slightly more difficult to utilize than

was the system (4.6)–(4.12); whereas the latter was reduced to a linear first order differential equation for one of the unknowns (A) as a function of y, the former could be reduced to coupled nonlinear first order differential equations for two of the unknowns. Solving the final pair of equations numerically and substituting the results into the remaining relations of the set would presumably yield improved functions $C_1(y)$, $C_2(y)$, and $C_3(y)$, particularly if the term in $(\lambda-\tfrac{1}{2})^{9/2}$ had been included in $G(\tfrac{1}{2}<\lambda<1/\sqrt{3})$. This would mean a better equation of state and, perhaps, satisfactory values of $(\partial g^{(2)}/\partial r_{12})_{r_{12}=a}$ and $(\partial^2 g^{(2)}/\partial r_{12}^2)_{r_{12}=a}$ at various densities. Finally, it should be noted that, for rigid spheres at least, superposition has been shown to be a surprisingly good approximation in the solid or dense fluid, even at $r_{12}=a$ (i.e., at contact between two spheres).[38]

In Sec. V, it was noted that even for our best choices of (λ_3, λ_4), the functions $G(\lambda)$ remain monotonic up to densities that are too high, are smoothly varying for all fixed $y<4$, display too shallow minima above $\lambda=1/\sqrt{3}$, and have slopes that are too small at $\lambda=1$. In addition, a maximum in $G(\lambda)$ just above $\lambda=1$, followed by a shallow minimum, was never obtained, although both these features should almost certainly be observed when y is very large. While some of the deficiencies in $G(\lambda\leq 1)$ could probably be eliminated in an extended theory using the superposition approximation and the jump in $\partial^4 G/\partial\lambda^4$ at $\lambda=1/\sqrt{3}$, it is clear that this approach would not produce the expected structure in $G(\lambda>1)$, since our functional form for $G(\lambda\geq 1/\sqrt{3})$ [i.e., (4.4)] is simply not flexible enough—even with another term added—to give a "trivacancy peak" near $\lambda=1$ as well as the "monovacancy peak" near $\lambda=1/\sqrt{3}$. In order to obtain the additional maximum and minimum, it might well be necessary to subdivide the interval $\lambda\geq 1/\sqrt{3}$, using an expansion about $\lambda=1/\sqrt{3}$ for $G(1/\sqrt{3}\leq\lambda<1)$ and a Laurent series or some modification thereof [such as (4.4) with λ_3 and/or λ_4 slightly less than unity] for $G(\lambda\geq 1)$. Although this option was considered and rejected for present purposes in Sec. IV, it is quite possible that the difficulties discussed there would have negligible physical consequences and that the use of the extra interval would, in fact, lead to an improved theory. Straightforward free area considerations indicate that G and its first nine derivatives with respect to λ are continuous at $\lambda=1$. This information, together with the integral and infinity conditions and the definition of C_1, would permit one to determine thirteen unknown functions of y distributed as "coefficients" among the functional forms chosen for $G(\tfrac{1}{2}\leq\lambda<1/\sqrt{3})$, $G(1/\sqrt{3}\leq\lambda<1)$, and $G(\lambda\geq 1)$, respectively.

So far, we have discussed two suggestions for extending our theory, both of which followed quite naturally from previous considerations. It is clear, however, that any scheme which provides additional exact information concerning $G(\lambda, y)$ and a means of incorporating it into the theoretical framework can be used as the basis for

such an extension. In particular, one possibly fruitful procedure is to introduce a new work quantity $Y(\lambda, y)$, defined to equal $W(\lambda, y)$ when $\lambda < \frac{1}{2}$ and to equal the reversible isothermal work required to form a certain type of fixed bicircular cavity in the system when $\lambda \geq \frac{1}{2}$. This cavity corresponds to the region that would be excluded to the centers of the rigid disks of diameter a by the presence of a fixed pair of rigid disks in contact, each with diameter $(2\lambda - 1)a$. The behavior of Y and some of its λ derivatives can be determined at $\lambda = \frac{1}{2}$ and $\lambda \approx 0.5476$, the point at which the bicircular region can first contain the centers of three disks of diameter a. Furthermore, a number of exact conditions relating Y, W, and G can be derived, among them

$$\beta(\partial Y/\partial \lambda)_{\lambda=1} = 2[\beta(\partial W/\partial \lambda)_{\lambda=1} - [G(1)]^{-1}(\partial G/\partial \lambda)_{\lambda=1}]$$ (6.1)

$$= 2[2yG(1, y) - [G(1, y)]^{-1}(\partial G/\partial \lambda)_{\lambda=1}],$$ (6.2)

which is of particular interest since it is the first relation involving $(\partial G/\partial \lambda)_{\lambda=1}$ that we have obtained. Although some of the new information would be needed to determine various "coefficients" appearing in expressions for $Y(\lambda)$, it is clear that this scheme would yield a net gain of several exact conditions on $G(\lambda, y)$, permitting one to adopt more flexible functional forms for that quantity in the various λ intervals.

With one of the extended theories just outlined, it might be possible to obtain an equation of state with a divergence at some density y^* close to $y_0 = 2\pi/\sqrt{3}$, together with functions $G(\lambda)$ with the proper non-monotonic behavior when y is large but not very near y^*. Using such approaches, however, it is not possible to produce a limit function similar to $G(\lambda, y_0)$, since if $A(y)$ diverges as $y \to y^*$, $G(\lambda, y^*)$ will not exist (i.e., will be infinitely large) for $\lambda \geq \frac{1}{2}$ (except possibly at a few isolated points). This is not necessarily a serious defect, since we are concerned primarily with densities in the range where the fluid–solid transition is believed to occur, not with densities near close packing.

The theory presented in Secs. III–V is a linear one, in the sense that only the first powers of A and C_1 appear in Eqs. (4.6)–(4.13). On the other hand, any extended theory utilizing the superposition approximation and the jump in $\partial^4 G/\partial \lambda^4$ at $\lambda = 1/\sqrt{3}$ will clearly be nonlinear, whether or not the interval $\lambda \geq 1/\sqrt{3}$ is subdivided or the quantity $Y(\lambda)$ is introduced. In a linear theory, $\pi a^2 \beta p(y)$ is an everywhere single-valued function of y, and a phase transition would be indicated by the presence of some unusual feature—probably something resembling a van der Waals loop—in this isotherm. With a nonlinear theory, however, it might be possible to obtain two distinct solutions to the particular system of simultaneous equations over some density range, one corresponding to a fluid and minimizing the Helmholtz free energy F at lower densities, the other

corresponding to a "solid" and minimizing F at higher densities.[39] The fluid→solid transition would then be located by equating the dimensionless pressures $\pi a^2 \beta p_1(y)$ and $\pi a^2 \beta p_2(y)$ and chemical potentials $\beta \mu_1(y)$ and $\beta \mu_2(y)$. Neither of the functions $\beta \mu_1(y)$ or $\pi a^2 \beta p_2(y)$ would have to do anything at all extraordinary at or near this transition, whereas in a successful linear theory, $\pi a^2 \beta p(y)$ would presumably have to change in a rather complicated manner over a narrow transition region in density. Intuitively, therefore, it seems that it might be easier to obtain a phase transition with a nonlinear theory than with a linear one.

Finally, it should be noted that if—instead of subdividing the interval $\lambda \geq \frac{1}{2}$—we were to use a Laurent series in nonpositive powers of λ for $G(\lambda \geq \frac{1}{2})$, determining the coefficients from the properties of the exact G at $\lambda = \frac{1}{2}$, the integral condition, and certain relations obtained from the statistical thermodynamics of curved interfaces, then it appears that inconveniently many terms would be needed to produce the complex behavior exhibited by $G(\lambda)$ at high densities.

ACKNOWLEDGMENT

APPENDIX A: $G(\lambda, \rho_0)$ FOR RIGID DISKS IN THE INTERVAL $1/\sqrt{3} < \lambda < 1$

When $1/\sqrt{3} < \lambda < 1$ and the number density ρ is slightly less than the close-packed density ρ_0, a λ-cule can be added to the rigid disk array in four different ways: it can be placed (1) in a monovacancy, (2) in a divacancy, (3) in a trivacancy or higher-order multiple vacancy, or (4) in an interstitial position. $G(\lambda, \rho)$ will be proportional to the average collision rate R of the λ-cule with its surroundings, which can be written

$$R = \sum_{i \geq 1} P_{iv} R_{iv} + (1 - \sum_{i \geq 1} P_{iv}) R_{int},$$ (A1)

$$P_{iv} = p_0^{(iv)}(\lambda)/p_0(\lambda),$$ (A2)

where R_{int} and R_{iv} are the average collision rates for a λ-cule in an interstitial position and in an i-disk vacancy, respectively, and $p_0^{(iv)}(\lambda)$ is the probability that a λ-cule, "tossed" into the assembly at random, will "land" in an i-disk vacancy ($i = 1$ for a monovacancy, 2 for a divacancy, etc.);

$$1 - \sum_{i \geq 1} P_{iv}$$

is, therefore, the conditional probability that the λ-cule, having been successfully placed at some arbitrary point in the system, lies in an interstitial position.

The ratios ρ_{jv}/ρ_{1v} ($j \geq 2$) of the densities of multiple vacancies to the density of monovacancies vanishes as $\rho \to \rho_0$ in such a way that, to leading order,[40]

$$\ln(\rho_{jv}/\rho_{1v}) = -(j-1)2/(\theta^{-1}-1),$$ (A3)

where θ is the reduced density ρ/ρ_0. Since each $p_0^{(iv)}$ contains a factor ρ_{iv} and both R_{1v} and R_{2v} remain finite as $\rho \to \rho_0$,[41] it is clear that the term $P_{2v}R_{2v}$ becomes vanishingly small in comparison to $P_{1v}R_{1v}$ as close packing is approached. Furthermore, although R_{jv} for $j \geq 3$ almost certainly diverges as $\rho \to \rho_0$ (see Appendix B), $P_{jv}R_{jv}/P_{1v}R_{1v}$ should still vanish in this limit since R_{jv} should diverge as some rather small power (quite possibly the first) of $(\theta^{-1}-1)^{-1}$, while $p_0^{(iv)}/p_0^{(1v)}$ will contain the very strongly vanishing factor $\exp[-(j-1)2/(\theta^{-1}-1)]$. Equation (A1) can, therefore, be simplified to

$$R = P_{mv}R_{mv} + (1-P_{mv})R_{int}, \quad (A4)$$

where the subscript mv denotes a monovacancy.

In a perfect rigid disk "crystal" with a density ρ slightly less than ρ_0, the average distance d between the centers of neighboring particles will slightly exceed the disk diameter a. Since

$$\theta^{-1} = (d/a)^2 = [1+(d-a)/a]^2 \cong 1+2(d-a)/a, \quad (A5)$$

it follows that

$$[(d-a)/a] \cong \tfrac{1}{2}(\theta^{-1}-1). \quad (A6)$$

In order to insert a λ-cule interstitially at some point in such a slightly expanded array, a large number of surrounding disks must give up some of their linear freedom of motion (essentially $d-a$). If each of these loses a finite fraction of its initial "play," then counting along a line of successive neighbors in the "crystalline" array, a number of disks proportional to $(\theta^{-1}-1)^{-1} \times (\lambda-1/\sqrt{3})$ will be involved, and the total number $n(\lambda)$ of disks affected by the addition of the λ-cule will be given by

$$n(\lambda) \cong K(\theta^{-1}-1)^{-2}(\lambda-1/\sqrt{3})^2, \quad (A7)$$

where K is a constant. Because we suppose that each of these $n(\lambda)$ particles loses some finite fraction of its free area, the free energy of formation of the interstitial "site" will, in the free area approximation, be

$$\frac{F_{int}(\lambda)}{kT} = \sum_{j=1}^{n(\lambda)} \ln \left[\frac{\text{initial free area}}{\text{free area after adding } \lambda\text{-cule}} \right] \quad (A8)$$

$$\cong K' \frac{(\lambda-1/\sqrt{3})^2}{(\theta^{-1}-1)^2}. \quad (A9)$$

(K' is a constant.) The average collision rate R_{int}, being a surface stress quantity for the λ-cule, is obtained from the λ derivative of (A9). Hence

$$R_{int}(\lambda) = f(\lambda)(\theta^{-1}-1)^{-2}a^{-1}(kT/m)^{1/2}, \quad (A10)$$

where $f(\lambda)$ is independent of θ and is finite throughout $1/\sqrt{3} < \lambda < 1$. In contrast to (A9) and (A10), respectively, the work of formation of a monovacancy diverges only as $2kT(\theta^{-1}-1)^{-1}$ as $\theta \to 1$ [16] and R_{mv} can be approximated roughly by $a^{-1}(kT/m)^{1/2}$, since a λ-cule in a monovacancy can "rattle around" rather freely. For ρ very

near ρ_0, therefore,

$$P_{mv} \cong 1,$$

$$1 - P_{mv} \cong \exp\{-K''[(\lambda-1/\sqrt{3})/(\theta^{-1}-1)]^2 + 2(\theta^{-1}-1)^{-1}\}, \quad (A11)$$

and (A4) becomes

$$R(\lambda) \cong R_{mv}(\lambda) + a^{-1}(kT/m)^{1/2}f(\lambda)(\theta^{-1}-1)^2$$
$$\times \exp\{-K''[(\lambda-1/\sqrt{3})/(\theta^{-1}-1)]^2 + [2/(\theta^{-1}-1)]\}. \quad (A12)$$

The second term on the right vanishes strongly as $\theta \to 1$, implying that $R(\lambda)$, and hence $G(\lambda)$, is determined in that limit exclusively by the monovacancy contribution. Interstitial addition is far too costly in terms of free energy to be a significant process.

Finally, it should be emphasized that the preceding arguments are not, in any sense, rigorous. We believe, however, that they leave little practical doubt that the contributions from multiple vacancies and interstitial positions can safely be neglected when determining $G(\lambda, \rho_0)$ for $1/\sqrt{3} < \lambda < 1$.

APPENDIX B: RELAXATION OF A RIGID DISK "CRYSTAL" INTO A TRIVACANCY

In Sec. II, it was argued that a λ-cule placed in a trivacancy in a rigid disk "crystal" should experience a divergent inward mean force in the limit $\rho \to \rho_0$, a result which seems to be clearly correct, intuitively, yet extremely difficult, if not impossible, to prove. In this appendix, we present a more detailed heuristic argument, based on the free area approximation, leading to the same conclusion. This is, however, merely an elaboration of the relevant portion of Sec. II, and certainly does not constitute a rigorous proof.

Figure 14 shows a λ-cule within a trivacancy in a nearly close-packed rigid disk assembly. When $\lambda < 2/\sqrt{3}$, the upper limit for trivacancy occupation, the three nearest neighbors (labeled with 1's) are free to slide inward; the pairs $(2, 2')$ can then move in and apart, followed by similar motions of the pairs $(3, 3')$. The fourth nearest neighbors can then move singly, followed by the fifth nearest neighbors, etc. This process will continue until the optimal relaxation (in terms of free energy) for the imperfect "crystal" is attained.

Let n_j be the number of jth nearest neighbors to the trivancy. ($n_1 = 3$, $n_2 = 6$, $n_3 = 6$, $n_4 = 3$, $n_5 = 6$, etc.) The added free area Δa_j available to a jth neighbor after the relaxation should be proportional to some power of $(2/\sqrt{3} - \lambda)$; i.e.,

$$\Delta a_j = A_j(2/\sqrt{3} - \lambda)^{p_j}, \quad (B1)$$

where $A_j \geq 0$ and $p_j > 0$. Actually, we expect that p_j should be ≥ 2 and may increase with increasing j due to cooperative effects. If the relaxation involves neighbors only through Nth order, then, in the free area approxi-

mation,[42]

$$\frac{F(\lambda)}{kT} = -\sum_{j=1}^{N(\lambda,\rho)} p_j n_j \ln \left[A_j{}^{1/p_j} \left(\frac{2}{\sqrt{3}} - \lambda \right) \right] \quad (B2)$$

and

$$(kT)^{-1} \frac{\partial F(\lambda)}{\partial \lambda} = [(2/\sqrt{3}) - \lambda]^{-1} \sum_{j=1}^{N(\lambda,\rho)} p_j n_j, \quad (B3)$$

where $F(\lambda)$ is the free energy of relaxation and $\partial F/\partial \lambda$ is just $\partial W^{(tv)}/\partial \lambda$ (see Sec. II), which is proportional to the average collision rate of the λ-cule with its neighbors and to $G(\lambda, \rho)$ in the interval $1 < \lambda < 2/\sqrt{3}$. A rather crude free area argument very similar to that used to obtain Eq. (A7) predicts that $N(\lambda, \rho)$ and hence $\partial F/\partial \lambda$ will diverge roughly as $(\theta^{-1} - 1)^{-1}$ as $\theta = \rho/\rho_0 \to 1$. Despite the lack of elegance or rigor, this indicates very persuasively that the λ-cule should experience an infinite inward mean force and infinite average collision rate R_{tv} in the limit of close packing, but that R_{tv} should diverge, at worst, as some fairly small power of $(\theta^{-1} - 1)^{-1}$.[43] If this is so, then it is clear that R_{iv} for $i \geq 4$ will also diverge as $\rho \to \rho_0$, since the disks surrounding higher-order multiple vacancies, like the neighbors of a trivacancy, are not locked into place by the remainder of the array.

APPENDIX C: SINGULARITY IN $G(\lambda)$ AT $\lambda = 1/\sqrt{3}$

When $\lambda \leq 1/\sqrt{3}$, all of the F_m in Eq. (3.4) vanish with the exception of F_1 and F_2. In the subsequent range $1/\sqrt{3} < \lambda \leq 1/\sqrt{2}$, three nonoverlapping disks can simultaneously have their centers within circular region $R(\lambda)$ with radius λa [see Eq. (3.3)], so then F_3 will be nonzero as well. Written explicitly, F_3 has the form

$$F_3 = (\tfrac{1}{6}\rho^3) \int_{R(\lambda)} d\mathbf{r}_1 \int_{R(\lambda)} d\mathbf{r}_2 \int_{R(\lambda)} d\mathbf{r}_3 g^{(3)}(\mathbf{r}_1, \mathbf{r}_2, \mathbf{r}_3). \quad (C1)$$
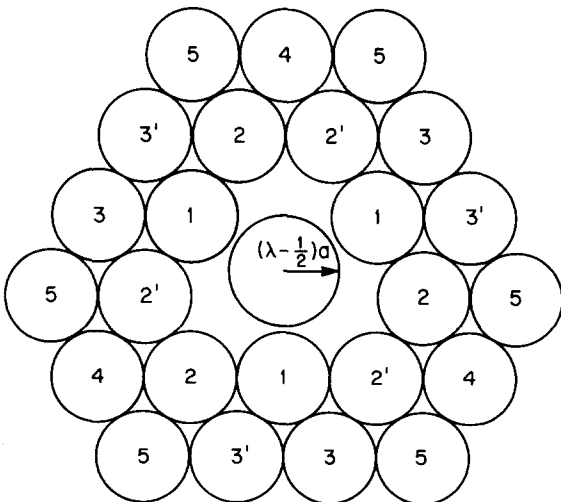

FIG. 14. A λ-cule within a trivacancy in the highly compressed rigid disk array ($\rho \to \rho_0$). The first through fifth nearest neighbors are labeled.
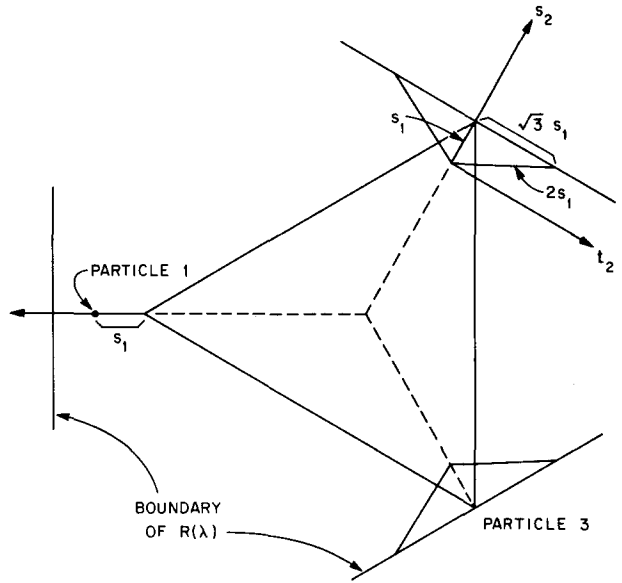

FIG. 15. Schematic drawing of the small isosceles triangles to which disks 2 and 3 are confined, when 1 is fixed and $\lambda - (1/\sqrt{3})$ is small. The bases are portions of the boundary of $R(\lambda)$, and the movable sides are generated by the singular rigid disk interactions. The specific side positions shown for particules 2 and 3 are the respective outermost limit consistent with given s_1.

Our objective is to deduce the leading-order behavior of $F_3(\lambda, \rho)$ as λ just begins to exceed $1/\sqrt{3}$. In this regime the disk centers at $\mathbf{r}_1$, $\mathbf{r}_2$, and $\mathbf{r}_3$ are tightly constrained so as to form nearly an equilateral triangle, so $g^{(3)}$ in Eq. (C1) will never deviate significantly from its triple contact value $g^{(3)}(a, a, a)$. Furthermore there are two independent and equivalent disk configurations, depending on whether $\mathbf{r}_1$, $\mathbf{r}_2$, $\mathbf{r}_3$ occur serially in clockwise or in counterclockwise order at the periphery of $R(\lambda)$. To the requisite order therefore,

$$F_3 = (\rho^3/3) g^{(3)}(a, a, a) \int_{T(\lambda)} d\mathbf{r}_1 d\mathbf{r}_2 d\mathbf{r}_3, \quad (C2)$$

where six-dimensional region $T(\lambda)$ constrains nonoverlapping disks 1, 2, and 3 to the clockwise ordering.

Particle 1 has the full polar angle $0 \leq \theta_1 \leq 2\pi$ available to its center, measured from the center of circle $R(\lambda)$. However the corresponding radial coordinate r_1 will have narrow limits, which to leading order in $\lambda - (1/\sqrt{3})$ will be

$$(a/\sqrt{3}) - 2a[\lambda - (1/\sqrt{3})] \leq r_1 \leq \lambda a. \quad (C3)$$

We may immediately carry out the θ_1 integration to transform (C2) to the following:

$$F_3 = [2\pi\rho^3 a/3\sqrt{3}] g^{(3)}(a, a, a)$$
$$\times \int_{(\sqrt{3}-2\lambda)a}^{\lambda a} dr_1 \int_{U(r_1,\lambda)} d\mathbf{r}_2 d\mathbf{r}_3, \quad (C4)$$

wherein $U(r_1, \lambda)$ is the appropriate four-dimensional region for disk centers $\mathbf{r}_2$ and $\mathbf{r}_3$.

On account of the minimal particle freedom of motion that obtains for small $\lambda - (1/\sqrt{3})$, the bounding arcs experienced by particles 2 and 3 (when 1 is fixed) have

negligible curvature. As shown schematically in Fig. 15, particles 2 and 3 then reside in small isosceles triangles with apex angles $2\pi/3$. The precise positions of the triangle sides for a given particle of course depend on the placement of the other two.

It is convenient to introduce (see Fig. 15) the reduced coordinate

$$s_1 = (r_1/a) - 2\lambda + \sqrt{3} \tag{C5}$$

to locate the radial position of particle 1. Similarly, reduced orthogonal coordinates s_2 and t_2 may be employed to measure the radial and tangential position of particle 2 in units a. As shown in Fig. 15, the origin for s_2 and t_2 is the innermost apex position consistent with the given s_1 value; hence s_2 is confined between limits 0 and s_1. Subsequently one sees that F_3 has the form

$$F_3 = \frac{2\pi\rho^3 a^6}{3\sqrt{3}} g^{(3)}(a, a, a)$$

$$\times \int_0^{3\lambda-\sqrt{3}} ds_1 \int_0^{s_1} ds_2 \int_{-\sqrt{3}s_2}^{\sqrt{3}s_2} dt_2 A(s_1, s_2, t_2), \tag{C6}$$

where $A(s_1, s_2, t_2)$ is the area (in units a^2) of the isosceles triangle available to 3 when 1 and 2 are fixed.

One easily finds that

$$A(s_1, s_2, t_2) = (\sqrt{3}s_2 - t_2)^2/4\sqrt{3}. \tag{C7}$$

This allows us to conclude from Eq. (C6) that the leading behavior of F_3 near $\lambda = 1/\sqrt{3}$ must be

$$F_3(\lambda, \rho) = 0 \qquad (\lambda \leq 1/\sqrt{3}),$$

$$= (27\sqrt{3}\pi/5)(\rho a^2)^3 g^{(3)}(a, a, a)[\lambda - (1/\sqrt{3})]^5$$

$$+ O\{[\lambda - (1/\sqrt{3})]^6\} \qquad \lambda \geq 1/\sqrt{3}. \tag{C8}$$

The sudden change in functional form implies, through Eq. (3.4), that the fifth λ derivative of $p_0(\lambda)$ suffers a simple discontinuity at $1/\sqrt{3}$ by an amount proportional to the mutual contact triplet distribution function. The identity (1.2) requires in turn that the fourth λ derivative of $G(\lambda)$ have a simple discontinuity at the same point $\lambda = 1/\sqrt{3}$, the lower derivatives being continuous there. Specifically,

$$G(1/\sqrt{3} \leq \lambda < 1/\sqrt{2}) = G(\tfrac{1}{2} \leq \lambda < 1/\sqrt{3})$$

$$+ \frac{81}{2\pi^2} \frac{y^2}{(1-\tfrac{1}{4}y)} \exp\left[2y \int_{1/2}^{\lambda} \lambda' G(\tfrac{1}{2} \leq \lambda' < 1/\sqrt{3}) d\lambda'\right]$$

$$\times g^{(3)}(a, a, a, \rho)[\lambda - (1/\sqrt{3})]^4 + O\{[\lambda - (1/\sqrt{3})]^5\}, \tag{C9}$$

and, therefore, the jump in $\partial^4 G/\partial\lambda^4$ at $\lambda = 1/\sqrt{3}$ is given by

$$\lim_{\lambda \to (1/\sqrt{3})^+} \left(\frac{\partial^4 G}{\partial\lambda^4}\right) - \lim_{\lambda \to (1/\sqrt{3})^-} \left(\frac{\partial^4 G}{\partial\lambda^4}\right) = \frac{972}{\pi^2} \frac{y^2}{(1-\tfrac{1}{4}y)}$$

$$\times \exp\left[2y \int_{1/2}^{1/\sqrt{3}} \lambda G(\tfrac{1}{2} \leq \lambda < 1/\sqrt{3})^- d\lambda\right] g^{(3)}(a, a, a, \rho). \tag{C10}$$

APPENDIX D: $\zeta_0, \zeta_1, \zeta_2, T_1, T_2, T_3, T_4, W_3,$ AND W_4 AS FUNCTIONS OF λ_3 AND λ_4

In this appendix we shall display the quite complicated dependences of the nine coefficients $\zeta_0, \zeta_1, \zeta_2, T_1, T_2, T_3, T_4, W_3,$ and W_4 on the parameters λ_3 and λ_4. First, however, let us define the following quantities:

$$\gamma_1 = \frac{1}{(1/\sqrt{3}-\lambda_3)^3} + \frac{(104/9)\sqrt{3}-20}{(1/\sqrt{3}-\lambda_3)^6} + \frac{18-(57/5)\sqrt{3}}{(1-\lambda_3)^3},$$

$$\gamma_2 = \frac{-3}{(1/\sqrt{3}-\lambda_3)^4} + \frac{140-80\sqrt{3}}{3(1/\sqrt{3}-\lambda_3)^6} + \frac{24\sqrt{3}-39}{(1-\lambda_3)^3},$$

$$\gamma_3 = \frac{12}{(1/\sqrt{3}-\lambda_3)^5} + \frac{40\sqrt{3}-60}{(1/\sqrt{3}-\lambda_3)^6} + \frac{54-42\sqrt{3}}{(1-\lambda_3)^3},$$

$$\delta_1 = \frac{1}{(1/\sqrt{3}-\lambda_4)^4} + \frac{(208/9)\sqrt{3}-40}{(1/\sqrt{3}-\lambda_4)^7} + \frac{18-(57/5)\sqrt{3}}{(1-\lambda_4)^4},$$

$$\delta_2 = \frac{-4}{(1/\sqrt{3}-\lambda_4)^5} + \frac{280-160\sqrt{3}}{(1/\sqrt{3}-\lambda_4)^7} + \frac{24\sqrt{3}-39}{(1-\lambda_4)^4},$$

$$\delta_3 = \frac{20}{(1/\sqrt{3}-\lambda_4)^6} + \frac{80\sqrt{3}-120}{(1/\sqrt{3}-\lambda_4)^7} + \frac{54-42\sqrt{3}}{(1-\lambda_4)^4},$$

$\Gamma_1 = \gamma_1 - (\delta_1/\delta_3)\gamma_3,$ $\qquad \Gamma_3 = 39 - 24\sqrt{3} + (52-42\sqrt{3})(\delta_2/\delta_3),$

$\Gamma_2 = \gamma_2 - (\delta_2/\delta_3)\gamma_3,$ $\qquad \Gamma_4 = (32/\pi)(1/\sqrt{3}-\tfrac{1}{2})^{1/2}[\tfrac{2}{3} - (2\sqrt{3}+3)(\delta_2/\delta_3)],$

$Q_1 = (57/5)\sqrt{3} - 18 + (54-42\sqrt{3})(\delta_1/\delta_3) - [39-24\sqrt{3}+(54-42\sqrt{3})(\delta_2/\delta_3)](\Gamma_1/\Gamma_2),$

$Q_2 = (32/\pi)(1/\sqrt{3}-\tfrac{1}{2})^{1/2}\{\tfrac{1}{5}(\tfrac{2}{3}\sqrt{3}-1) - (2\sqrt{3}+3)(\delta_1/\delta_3) - [\tfrac{2}{3} - (2\sqrt{3}+3)(\delta_2/\delta_3)](\Gamma_1/\Gamma_2)\},$

$$Q_3 = \tfrac{7}{2} - 2\sqrt{3} - \tfrac{3.5}{2}(\delta_1/\delta_3) + 7[1 - \tfrac{2}{3}\sqrt{3} + \tfrac{5}{2}(\delta_2/\delta_3)](\Gamma_1/\Gamma_2),$$

$$\Omega_1 = \frac{\tfrac{2}{3}\sqrt{3} - \lambda_3}{(1/\sqrt{3} - \lambda_3)^2} + \frac{[(2360/567) - (584/243)\sqrt{3}]}{(1/\sqrt{3} - \lambda_3)^6} - \frac{(2-\lambda_3)}{(1-\lambda_3)^2} + \frac{(382/135)\sqrt{3} - (362/63)}{(1-\lambda_3)^3},$$

$$\Omega_2 = \frac{\sqrt{3} - \lambda_4}{3(1/\sqrt{3} - \lambda_4)^3} + \frac{(4720/567) - (1168/243)\sqrt{3}}{(1/\sqrt{3} - \lambda_4)^7} - \frac{(1 - \tfrac{1}{3}\lambda_4)}{(1-\lambda_4)^3} + \frac{(382/135)\sqrt{3} - (362/63)}{(1-\lambda_4)^4},$$

$$\Omega_3 = (7\Omega_1/\delta_3)[\tfrac{5}{2} + [1 - \tfrac{2}{3}\sqrt{3} + \tfrac{5}{2}(\delta_2/\delta_3)](\gamma_3/\Gamma_2)] - (7\Omega_2/\Gamma_2)[1 - \tfrac{2}{3}\sqrt{3} + \tfrac{5}{2}(\delta_2/\delta_3)] + (659/891) - (380/891)\sqrt{3}.$$

In terms of the above functions of λ_3 and λ_4, the ζ's, T's, and W's can be written

$$\zeta_0 = \frac{764}{135}\sqrt{3} - \frac{661}{63} + 2\left[\frac{\Gamma_3}{\Gamma_2}\Omega_1 + \left(42\sqrt{3} - 54 - \frac{\Gamma_3}{\Gamma_2}\gamma_3\right)\frac{\Omega_2}{\delta_3} - \frac{Q_1}{Q_3}\Omega_3\right],$$

$$\zeta_1 = \frac{647}{84} - \frac{191\sqrt{3}}{45} + \frac{(1/\sqrt{3} - \tfrac{1}{2})^{1/2}}{\pi}\left(\frac{7809}{8505}\sqrt{3} - \frac{4416}{2835}\right) + (\Gamma_4 - \tfrac{3}{2}\Gamma_3)\frac{\Omega_1}{\Gamma_2}$$

$$+ \left[\frac{16}{\pi}(1/\sqrt{3} - \tfrac{1}{2})^{-1/2} + 81 - 63\sqrt{3} + (\tfrac{3}{2}\Gamma_3 - \Gamma_4)\frac{\gamma_3}{\Gamma_2}\right]\frac{\Omega_2}{\delta_3} + (\tfrac{3}{2}Q_1 - Q_2 - 1)\frac{\Omega_3}{Q_3},$$

$$\zeta_2 = \frac{191}{270}\sqrt{3} - \frac{80}{63} + \frac{\Gamma_3}{\Gamma_2}\frac{\Omega_1}{4} + \left(42\sqrt{3} - 54 - \frac{\Gamma_3}{\Gamma_2}\gamma_3\right)\frac{\Omega_2}{4\delta_3} + \frac{(1-Q_1)}{4Q_3}\Omega_3,$$

$$T_1 = \tfrac{3}{4}\zeta_0 + \zeta_1 + \tfrac{1}{4}$$

$$T_2 = \tfrac{1}{4}T_1 + \frac{4}{27}\sqrt{3} - \tfrac{1}{4} + 2\left[\frac{\Omega_1}{\Gamma_2} - \frac{\gamma_3}{\delta_3}\frac{\Omega_2}{\Gamma_2} + \left(\frac{\Gamma_1}{\Gamma_2} - \tfrac{1}{3}\sqrt{3} + \tfrac{1}{2}\right)\frac{\Omega_3}{Q_3}\right],$$

$$W_3 = \frac{37}{144} - \frac{4}{27}\sqrt{3} + 4\left(\tfrac{1}{3}\sqrt{3} - \tfrac{1}{2} - \frac{\delta_2}{\delta_3}\right)\frac{\Omega_1}{\Gamma_2} + 4\left[\Gamma_2 + \left(\tfrac{1}{2} - \tfrac{1}{3}\sqrt{3} + \frac{\delta_2}{\delta_3}\right)\gamma_3\right]\frac{\Omega_2}{\Gamma_2\delta_3}$$

$$+ 2\left[\frac{2}{\delta_3}\left(\delta_1 - \frac{\Gamma_1}{\Gamma_2}\delta_2\right) + (\tfrac{2}{3}\sqrt{3} - 1)\frac{\Gamma_1}{\Gamma_2} + \tfrac{1}{3}\sqrt{3} - \tfrac{7}{12}\right]\frac{\Omega_3}{Q_3},$$

$$T_3 = \tfrac{9}{8}W_3 + T_2/4 - T_1/16,$$

$$W_4 = 3\left(\frac{225\,283}{362\,880} - \frac{871}{2430}\sqrt{3} + \left[(4\sqrt{3} - \tfrac{13}{2})\frac{\delta_2}{\delta_3} + \tfrac{7}{2}\sqrt{3} - \tfrac{73}{12}\right]\frac{\Omega_1}{\Gamma_2} - \left\{(4\sqrt{3} - \tfrac{13}{2})\Gamma_2 + \left[(4\sqrt{3} - \tfrac{13}{2})\frac{\delta_2}{\delta_3} + \tfrac{7}{2}\sqrt{3} - \tfrac{73}{12}\right]\gamma_3\right\}\frac{\Omega_2}{\Gamma_2\delta_3}\right.$$

$$\left. - \left[(4\sqrt{3} - \tfrac{13}{2})\frac{(\delta_1 - \Gamma_1\delta_2/\Gamma_2)}{\delta_3} + (\tfrac{73}{12} - \tfrac{7}{2}\sqrt{3})\frac{\Gamma_1}{\Gamma_2} + \frac{139}{48} - \frac{301}{180}\sqrt{3}\right]\frac{\Omega_3}{Q_3}\right)$$

$$T_4 = \tfrac{1}{3}W_4 + \tfrac{5}{32}W_3.$$

[1] H. Reiss, H. L. Frisch, and J. L. Lebowitz, J. Chem. Phys. **31**, 369 (1959).

[2] E. Helfand, H. L. Frisch, and J. L. Lebowitz, J. Chem. Phys. **34**, 1037 (1961).

[3] J. L. Lebowitz, E. Helfand, and E. Praestgaard, J. Chem. Phys. **43**, 774 (1965).

[4] A. B. Ritchie, J. Chem. Phys. **46**, 618 (1967).

[5] R. M. Gibbons, Mol. Phys. **17**, 81 (1969).

[6] M. A. Cotter and D. E. Martire, J. Chem. Phys. **52**, 1902, 1909 (1970); **53**, 4500 (1970).

[7] G. Lasher, J. Chem. Phys. **53**, 4141 (1970).

[8] K. Timling, Philips Research Rept. **25**, 223 (1970).

[9] E. Helfand, H. Reiss, and H. L. Frisch, J. Chem. Phys. **33**, 1379 (1960).

[10] F. H. Stillinger and M. A. Cotter, J. Chem. Phys. **55**, 3449 (1971).

[11] M. S. Wertheim, Phys. Rev. Letters **10**, 321 (1963); E. Thiele, J. Chem. Phys. **38**, 1959 (1963).

[12] For a review and discussion of the available numerical results (from both Monte Carlo and molecular dynamics calculations) for the rigid disk system, see W. W. Wood, in *Physics of Simple Liquids*, edited by H. N. V. Temperley, J. L. Rowlinson, and G. S. Rushbrooke (Interscience, New York, 1968), Chap. 5, pp. 163–184.

[13] D. M. Tully-Smith and H. Reiss, J. Chem. Phys. **53**, 4015 (1970).

[14] H. Reiss and D. M. Tully-Smith, J. Chem. Phys. **55**, 1674 (1971).

[15] An exclusion cavity of radius λa is equivalent to the presence of a scaled disk of diameter $b = (2\lambda - 1)a$, and for $\lambda < \tfrac{1}{2}$, $b < 0$. Within the framework of scaled particle theory, negative b corresponds to a point particle which can penetrate a disk of diameter a to a distance $|b|/2$ normal to its surface.

[16] F. H. Stillinger, Jr., Z. W. Salsburg, and R. L. Kornegay, J. Chem. Phys. **43**, 932 (1965).

[17] Because of the lack of true long-range translational order in two dimensions, the singlet distribution function $\rho^{(1)}$ is independent of position in the thermodynamic limit; i.e., $\rho^{(1)} = \rho = N/V$ at all densities. Thus Eq. (3.1) is valid for the "solid" as well as the fluid phase of the rigid disk system. In contrast to this, the three-dimensional analogue of (3.1), $p_0(\lambda, \rho) = 1 - \tfrac{4}{3}\pi\rho a^3\lambda^3$, would be valid for a rigid sphere crystalline phase only if ρ were set equal to the unit cell average of the oscillatory $\rho^{(1)}(\mathbf{r}_1)$.

[18] As was noted by RFL, their Eq. (3.11) is just a special case

of Eq. (60) of J. E. Mayer and E. Montroll, J. Chem. Phys. **9**, 2 (1941).

[19] T. L. Hill, *Statistical Mechanics* (McGraw-Hill, New York, 1956), Sec. 29.

[20] In the rigid disk "solid," the pair correlation function $g^{(2)}$ depends not only on $|r_{12}|$, but also on the angle θ_{12} between r_{12} and some specified spatial direction. ($g^{(2)}$ does not depend on r_1 and r_2 individually because of the lack of true long-range order.) Since $R(\lambda)$ is a circle, however, (3.7) and all subsequent equations in this section will be valid for the "solid" if we take $g^{(2)}(r_{12}, \rho)$ to mean the angular average of $g^{(2)}(r_{12}, \theta_{12}, \rho)$. ($r_{12} = |r_{12}|$.)

[21] The continuity of $G(\lambda)$ and $\partial G/\partial \lambda$ at $\lambda = \frac{1}{2}$, together with the divergence of $\partial^2 G/\partial \lambda^2$ there, were already noted by HFL. [They incorrectly stated, however, that the second derivative diverges as $(\lambda - \frac{1}{2})^{-1}$.] The new information in Sec. III consists of (1) the behavior of G and its lower-order λ derivatives at $\lambda = 1/\sqrt{3}$; (2) the actual exhibition of the first three terms in the expansions of p_0 and G about $\lambda = \frac{1}{2}$.

[22] A straightforward free area argument can be used to show that the first λ derivative of G to show a discontinuity at $\lambda = 1/\sqrt{2}$ is $\partial^6 G/\partial \lambda^6$, while at $\lambda = [2/(5 - 5^{1/2})]^{1/2}$, it is $\partial^8 G/\partial \lambda^8$.

[23] Such square and pentagonal arrangements do not occur in an undistorted hexagonal array; therefore, the weak singularities at $\lambda = 1/\sqrt{2}$ and $\lambda = [2/5 - 5^{1/2}]^{1/2}$ probably have very little effect on the behavior of the rigid disk "solid." This may not be the case, however, for the moderately dense fluid.

[24] Strictly speaking, $G(\lambda, y)$ and $G(\lambda, \rho)$ should not be used interchangeably, since G does not have the same functional dependence on y as on ρ. Both symbols, however, are intended to denote a quantity—the contact pair correlation function—which depends on λ and ρ or y, not functional forms. This slight imprecision should not, we believe, create any confusion. Use of rigorously correct notation would be unnecessarily cumbersome.

[25] Equations (4.18) and (4.21) are only valid when $|\zeta_1|/q < 1$ and when $|\zeta_1|/q^* > 1$, respectively. When $\zeta_0 > 0$, $q^2 > 0$, and $|\zeta_1|/q > 1$, $A(y)$ is given by (4.18) with $(q - \zeta_1 - 2\zeta_2 y)$ and $(q - \zeta_1 - 2\zeta_2 y')$ replaced by $(\zeta_1 - q + 2\zeta_2 y)$ and $(\zeta_1 - q + 2\zeta_2 y')$. On the other hand, when $\zeta_0 < 0$, $q^2 > 0$, and $|\zeta_1|/q^* < 1$, $(\zeta_1 - q^* + 2\zeta_2 y)$ must be replaced by $(q^* - \zeta_1 - 2\zeta_2 y)$, in (4.21). These two cases do not occur, however, for any pairs of parameters (λ_3, λ_4) with which we shall be concerned.

[26] When $\zeta_0 < 0$, it is clear that the solution to (4.16) can no longer be expressed in terms of a definite integral with $y = 0$ as its lower limit. Hence, we have used indefinite integrals to represent those classes of functions whose derivatives are given by the integrands in (4.21) and (4.22), respectively.

[27] Z. Kopal, *Numerical Analysis* (Wiley, New York, 1961), Sec. IV-L.

[28] Equations (5.3) and (5.6) could actually be used to calculate $A(y)$. One would need to use a lower limit y_l small enough so that $A(y_l)$ could be determined with sufficient accuracy from the virial expansion truncated after a few terms, yet large enough so that serious losses of significant figures would not occur during the computations. (With a very small y_l, the integral and C_l are both very large and of opposite sign.) In practice, this balance is hard to achieve (without determining a large number of virial coefficients) and it is more convenient to use the Runge–Kutta method to solve (4.16) directly.

[29] Z. W. Salsburg and W. W. Wood, J. Chem. Phys. **37**, 798 (1962).

[30] B. J. Alder and T. E. Wainwright, as quoted in W. G. Hoover and B. J. Alder, J. Chem. Phys. **46**, 686 (1967).

[31] B. J. Alder and T. E. Wainwright, Phys. Rev. **127**, 359 (1962).

[32] The quantity $(W_4/3 - W_3/8)$ appearing in the last terms of the integrands in the expressions for $A(y)$ is negative. As a result, for pairs of parameters corresponding to points (λ_3, λ_4) in regions I, II, and IV, $A(y)$ goes through a maximum at y_m, then diverges as $-(1 - y/4)^{-3}$ as $y \to 4$. In most cases, $y_m > y_0$; in all cases, A is positive and large for all $y \leq y_0$. In region III, on the other hand, two different types of behavior occur: For some (λ_3, λ_4), $A(y)$ monotonically increases from $y = 0$ to $y = y_+$, diverging to $+\infty$ as $y \to y_+$; at other points, it goes through a maximum at some y_m then diverges to $-\infty$ as $y \to y_+$.

[33] F. H. Ree and W. G. Hoover, J. Chem. Phys. **46**, 4181 (1967).

[34] The notation $\Delta \phi(y | \lambda_3, \lambda_4)$ and $A(y | \lambda_3, \lambda_4)$ is intended to signify that $\Delta \phi$ and A are functions of a single variable y, while λ_3 and λ_4 are to be regarded as parameters.

[35] F. H. Ree and W. G. Hoover, J. Chem. Phys. **40**, 939 (1964).

[36] By the "usable" parts of region III, we mean those portions of the region where physically reasonable functions $A(y | \lambda_3, \lambda_4)$ can be obtained.

[37] By substituting $G(\frac{1}{2} \leq \lambda < 1/\sqrt{3})$ from (4.1) into (C10), adding the result to $(\partial^4 G/\partial \lambda^4)_{\lambda = 1/\sqrt{3}}$ obtained from (4.1), equating the sum to $(\partial^4 G/\partial \lambda^4)_{\lambda = 1/\sqrt{3}}$ from (4.4), and rearranging, one can derive an expression for $g^{(3)}(a, a, a, \rho)$ in terms of the variable y and the functions $A(y)$, $B(y)$, $D(y)$, $E(y)$, $C_1(y)$, $C_2(y)$, and $C_3(y)$. This leads to unsatisfactory results, however, in that $g^{(3)}(a, a, a, \rho)$ does not approach unity as $\rho \to 0$.

[38] B. J. Alder, Phys. Rev. Letters **12**, 317 (1964).

[39] The only way to decide whether a given solution corresponds to a fluid or a "solid" is to examine the λ dependence of the contact pair correlation function. We expect G to be a monotonically increasing function of λ in a fluid, but to exhibit the sort of non-monotonic behavior discussed in Secs. II and V in a "solid."

[40] J. C. Langeberg and G. V. Bettoney, J. Phys. Chem. Solids (to be published).

[41] As stated previously, the disks surrounding a monovacancy are virtually locked into place at densities slightly less than ρ_0. Similarly, only two of the eight nearest neighbors of a divacancy are free to move inward, and after they do so, the other disks in the assembly remain essentially locked into position. Both R_{1v} and R_{2v} remain finite, therefore, as $\rho \to \rho_0$, since the surrounding "crystal" cannot strongly "crowd" a λ-cule present in a mono- or divacancy.

[42] The free area approximation yields expressions for the free energy and the equation of state of the rigid disk "solid" which can be shown to be asymptotically exact in the limit $\rho \to \rho_0$.[29] This asymptotic validity is believed to persist in the thermodynamic limit, but this cannot be proven rigorously.

[43] For λ slightly greater than unity, it could also be argued that R_{1v} should diverge as $\theta \to 1$ in roughly the same manner as does the pressure of the rigid disk assembly. As noted previously, the latter is believed to increase as $(1/\theta - 1)^{-1}$ very near close packing.